

Characterizing the Thermal Resistance of Alternating Current Light Emitting Diodes

by

Adikaramge Asiri Jayawardena

A Thesis Submitted to the Graduate

Faculty of Rensselaer Polytechnic Institute

In Partial Fulfillment of the

Requirements for the degree of

MASTER OF SCIENCE

Major Subject: Lighting

Approved by:

Nadarajah Narendran, Ph.D.
Thesis Adviser

Rensselaer Polytechnic Institute
Troy, New York
November 2011
(For Graduation in December 2011)

© Copyright 2011

by

Asiri Jayawardena

All Rights Reserved

CONTENTS

LIST OF TABLES.....	vi
LIST OF FIGURES	vii
ACKNOWLEDGMENT	ix
ABSTRACT	x
1. Background.....	1
2. Literature Review	3
2.1 Basics of LED	3
2.2 AC LED package	4
2.3 Junction Temperature.....	7
2.4 Measuring Junction Temperature of DC LEDs	7
2.4.1 Electrical test methods	8
2.4.2 Optical test methods.....	10
2.5 Measuring Junction Temperature of AC LEDs	11
2.5.1 RMS current recovery method.....	13
2.5.2 Voltage drop method for AC LED.....	15
2.6 Thermal resistance	16
2.7 Characterization of thermal resistance of DC LED packages.....	18
2.8 Summary of the literature review.....	20
3. Hypotheses.....	22
3.1 Hypothesis 1.....	22
3.2 Hypothesis 2.....	23
3.3 Hypothesis 3.....	23
3.4 Hypothesis 4.....	23
4. Experiment.....	25
4.1 Hypothesis 1: Comparison of measurement methods.....	25
4.1.1 Experiment Variables.....	25

4.1.2	Experiment set up: voltage drop method for AC LED	27
4.1.3	Experiment procedure: voltage drop method for AC LED	29
4.1.4	Experiment set up: rms current recovery method	33
4.1.5	Experiment procedure: rms current recovery method.....	34
4.1.6	Experiment procedure: the first half cycle heating	35
4.2	Hypothesis 2: peak wavelength shift method	39
4.2.1	Experiment variables.....	39
4.2.2	Experiment procedure: peak wavelength shift method.....	40
	Hypothesis 3: variation of thermal resistance with ambient temperature.....	42
4.2.3	Experiment variables.....	42
4.2.4	Experiment procedure	43
4.3	Hypothesis 4: Variation of thermal resistance with input voltage	44
4.3.1	Experiment variables.....	44
5.	Results.....	45
5.1	Verification of Hypothesis 1	45
5.2	Verification of Hypothesis 2	50
5.3	Verification of Hypotheses 3&4	53
6.	Discussion.....	56
6.1	Absolute junction temperature measurement.....	56
6.2	Measurement Uncertainty: voltage drop method.....	59
6.2.1	Calibration curve.....	59
6.2.2	Thermal environment	60
6.2.3	Pin temperature measurement	61
6.2.4	The uncertainty analysis.....	62
6.3	In line measurement of AC LED packages.....	63
7.	Conclusion	64
8.	Bibliography	66

Appendix A: Forward voltage drop method	73
Appendix B: Forward voltage recovery method	75
Appendix C: Pilot study to determine the uncertainty of the rms current recovery set-up	78
Appendix D: AC LED control circuit for voltage drop method for AC LED.....	80
Appendix E: Optical power measurement.....	82
Appendix F: Results of Samples measured	85
Appendix G: Uncertainty Analysis.....	92

LIST OF TABLES

Table 1: Estimated junction temperature of white AC LED package at 120V	46
Table 2: Thermal Resistance calculations using voltage drop method for AC LED.....	46
Table 3: First half cycle rms current measurements	46
Table 4: Thermal resistance calculation using rms current recovery method	47
Table 5: Junction Temperature after the first half cycle of AC current.....	48
Table 6: Thermal resistance calculated after accounting for first half cycle heating	48
Table 7: Comparison of thermal resistance values calculated using two methods.....	48
Table 8: Comparison of thermal resistance measurements for GaP LED.....	49
Table 9: Estimated junction temperature of GaP based AC LED package	51
Table 10: Peak wavelength of GaP based AC LED package	52
Table 11: Average of estimated junction temperature for Sample 1	53
Table 12: Thermal resistance of sample 1	53
Table 13: Comparison of junction temperature measurements using voltage drop and peak wavelength shift methods.....	59
Table 14: Standard errors of thermocouple types	61
Table 15: Summary of the uncertainty analysis	62
Table 16: Average of estimated junction temperature for Sample 1	85
Table 17: Electric input power for sample 1	86
Table 18: Optical power of sample 1.....	86
Table 19: Thermal resistance of sample 1	86
Table 20: Results of 3 by 3 F-test for sample 1	86
Table 21: Results of the T-test that compared the temperature points of sample 1.....	87
Table 22: Paired T-test for sample 1 at different input voltages	88
Table 23: Estimated Junction Temperature of sample 2	90
Table 24: Optical power of sample 2.....	90
Table 25: Electric input power of sample 2.....	90
Table 26: Thermal resistance of sample 2	90
Table 27: Results of F-test analysis for sample 2	91

LIST OF FIGURES

Figure 1: Band gap & electron-hole recombination process [17].....	4
Figure 2: The variation of relative output power and forward voltage with the number of dies in an AC LED package [22].....	5
Figure 3: Circuit diagram of a series LED array in an AC LED package [22]	6
Figure 4: AC LED with series type configuration.....	6
Figure 5: Circuit diagram of the Wheatstone Bridge configuration [6]	6
Figure 6: Relationship between first half cycle rms current and heat sink temperature [2]	13
Figure 7: Illustration of rms current recovery method [2].....	14
Figure 8: Reference current pulse (I_{ref}) is applied at the current dead-zone region [3]...	15
Figure 9: Junction temperature when reference pulse is applied at different phase angles of the voltage waveform [3].	16
Figure 10: Variation of thermal resistance with input power for 1W (a) and 5W (b) DC LED [46].....	19
Figure 11: Experiment set up for voltage drop method [3]	27
Figure 12: Voltage-current characteristics of a white AC LED	29
Figure 13: Calibration curve for white AC LED	31
Figure 14: Reference current pulse at the current dead-zone of the AC LED.....	32
Figure 15: Schematic diagram of the experiment setup for rms current recovery method	33
Figure 16: The reference current pulse at different phase angles of the first half cycle of AC voltage waveform.....	37
Figure 17: Heating profile of the string of junctions of an AC LED package at 120V at 75 ⁰ C during the first half cycle of the AC voltage waveform	38
Figure 18: Variation of Peak Wavelength with DC current of a GaP based AC LED package	41
Figure 19: Calibration curve for white AC LED sample.....	45
Figure 20: The comparison of thermal resistance measured using voltage drop method for AC LED and rms current recovery method before adjusting for first half cycle heating.....	49

Figure 21: The comparison of thermal resistance measured using voltage drop method for AC LED and rms current recovery method after adjusting for first half cycle heating	50
Figure 22: Calibration curve for GaP based AC LED package.....	51
Figure 23: Relationship between junction temperature and peak wavelength for GaP based AC LED package.....	52
Figure 24: Variation of thermal resistance with cold plate temperature of sample 1, GaN based white AC LED package.....	54
Figure 25: variation of thermal resistance with input AC voltage for sample1, GaN based white AC LED package	55
Figure 26: Calibration curve for peak wavelength shift method	56
Figure 27: Peak wavelengths vs. estimated T_j using voltage drop method for AC LED and peak wavelength shift method	57
Figure 28: Illustration of forward voltage drop method for DC LEDs [60].....	74
Figure 29: Forward voltage drop over time.....	76
Figure 30: Illustration of voltage recovery method [14].	77
Figure 31: Frist half cycle rms current Vs. pin temperature.....	78
Figure 32: The reference current pulse.....	81
Figure 33: Calibration factors used for integrating sphere calibration	82
Figure 34: Spectral power distribution of a white AC LED	83
Figure 35: Variation of optical power with temperature	84
Figure 36: Calibration curve for sample 1	85
Figure 37: Calibration curve for sample 2.....	89
Figure 38: Variation of thermal resistance with input AC voltage for sample 2.....	91

ACKNOWLEDGMENT

I would like to dedicate this thesis to the two women that I love most in my life, my mother and my grandmother. Thank you so much amma, for your unconditional love and for being such a strong source of inspiration at every step of my life. I'm so sad Loku that you are not there to see this day, but I'm sure that you're watching me from above and guiding me as you have always done. I would like to thank my father, my three sisters and my grandfather for being there for me always and helping me to become who I am today. I would also like to mention with gratitude my school, Marist Stella College my university, university of Moratuwa & my country, Sri Lanka for free education.

Thank you to my uncle, Tilak and Upali for introducing me to LRC and encouraging me to pursue my graduate studies. I'm ever so grateful to Narendran, my thesis advisor and mentor for the guidance you gave me and for pushing me to do that extra bit that made my experience at LRC so rewarding. I would like to thank John Bullough for spending time in reviewing my thesis and providing me with valuable feedback. I appreciate the contribution of Yiting Zhu in helping me with my experiments and for reviewing my thesis. I would like to thank my colleagues at LRC and specially Yi-wei Liu, Terry Klein & Kate Sweater for helping me in my research.

I would like to acknowledge the lighting research center for my graduate assistantship and for providing me with a resourceful & pleasant environment to pursue my research. I would also like to thank RPI for the opportunity to pursue graduate studies. I would like to acknowledge my sponsors FAA, Alliance for Solid State Illumination Systems & Technologies and Lite-on Inc. for supporting my research.

Finally I would like to thank God the almighty and my guardian angel for its blessings without any of these would have been possible.

ABSTRACT

Light-emitting diode (LED) operating on alternating current (AC) is gaining popularity in lighting applications. The junction temperature of an LED has a significant influence on its performance, including light output, spectrum, and reliability. Since junction temperature cannot be measured directly, most methods presently used with direct current (DC) LEDs are indirect, and provide estimations of junction temperature. Manufacturers specify the thermal resistance of a package with respect to an external reference point. This way, users could estimate the junction temperature in a particular application by measuring the temperature at this reference point.

Although there are many proven methods for estimating the junction temperature of DC LEDs, only a few methods have been proposed for AC LEDs [1,2,3,4]. Of these, two different methods were selected for further investigation and analysis to determine their accuracy in estimating the AC LED junction temperature. Liu et al. [3], used a low reference current pulse when the AC LED is not conducting to extract the voltage across the junction to estimate the junction temperature. Zong et al. [2], estimated the junction temperature by recovering the first half cycle root-mean-square (rms) current using an active heat sink. The measured thermal resistance values of an AC LED package using these two methods didn't agree [3]. Liu et al. [3], hypothesized that this discrepancy was due to the heating in the first half cycle of current that Zong et al. [2], did not account for in their method. However, no proof was given to validate this assumption.

In this thesis, several hypotheses were developed and verified using laboratory experiments. The results showed that by measuring and correcting for the temperature rise in the junction during the first half cycle of current, the thermal resistance values estimated using the two approaches agree.

In addition, a third method is described in which the peak wavelength value of the spectrum was used to estimate the junction temperature of a GaP (Gallium Phosphide) based AC LED package. The junction temperature values estimated using the peak wavelength shift method and voltage drop method for a GaP AC LED package is within

the measurement uncertainty of the two methods. The details of the methods, and the associated results, along with their accuracies are presented and discussed in the thesis.

Upon validating the accuracy of the voltage drop method, the thermal resistance of a GaN (Gallium Nitride) based white AC LED was characterized at different ambient temperature and input voltage conditions. The thermal resistance values of GaN AC LED samples measured using the voltage drop method showed an increase in thermal resistance when the ambient temperature increased. This behavior is consistent with the observed variation of thermal resistance to ambient temperature, for DC LEDs, in past studies. The thermal resistance showed a decreasing trend with increasing input voltage. This is consistent with past studies that show variation of thermal resistance in DC LEDs with high package series electrical resistance.

1. Background

Light emitting diode (LED) is a rapidly growing light source technology that has the potential to reduce lighting energy consumption [5]. An LED is a semiconductor P-N junction (P- high concentration of holes or positive charges; N- high concentration of electrons or negative charges). An LED generates light (photons) when the positive and negative charges combine radiatively. The fabrication of semiconductor packages with high optical emission efficiencies and better light extraction efficiencies has enabled LEDs to be used in general lighting applications. Heat generated at the junction is mainly a consequence of non-radiative recombination, extraction inefficiency and ohmic resistance.

In recent years, alternating current (AC) LEDs have entered the marketplace. The AC LED packages are fabricated by growing several junctions on an insulated substrate. The junctions are connected either in parallel or series, so that they could be directly connected to an AC power source [6]. AC LED packages do not require an AC to DC converter, and can be connected to an AC grid directly. The absence of a driver could reduce the overall system cost, increase reliability, and reduce the overall size of an LED luminaire. For these reasons, AC-LED technology has captured the interest of the LED lighting community.

The junction temperature of an LED has a significant influence on its efficiency, reliability and light output characteristics [7]. The reliability of semiconductor devices is often predicted using the junction temperature [8]. To design efficient and reliable LED lighting systems, it is critical to know the junction temperature of an LED in a given operating environment. It is practically impossible to obtain a direct measurement of the junction temperature. There are several methods that could be used to estimate the junction temperature of an LED [9,10,11,12,13,14,1,2,3]. The focus of these methods is to identify a measurable external parameter that has a close relationship with the junction temperature (ex: forward voltage, peak wavelength of the emission, etc.).

The users of LED packages rely on the thermal resistance value specified by manufacturers, between the junction and a measurable reference point, to estimate junction temperature. Thermal resistance measurement of a DC LED has been extensively studied [9,10,11,12,13]. However, there are only a few studies that discuss the junction temperature and thermal resistance measurement of AC LEDs [1,2,3,4].

In a study conducted at the Lighting Research Center (LRC), researchers developed a method for measuring the junction temperature of an AC LED and its thermal resistance [3]. In that study, LRC researchers measured the thermal resistance using another method, rms current recovery method, reported in literature for comparison [2]. The thermal resistance values measured using the two methods did not agree [3]. In that study, the authors hypothesized that the discrepancy was due to the additional heating in the first half cycle of current that Zong et al. [2], did not account for in their method. However, no proof was given to validate this assumption. The objective of this thesis is to investigate the reasons behind this discrepancy. Additionally, the thesis studied the thermal resistance values of an AC LED at different ambient temperatures and at different input voltages.

2. Literature Review

The literature review focused on the basics of LEDs, AC LED packages, junction temperature (T_j) prediction methods for DC and AC LEDs, and characterization of the thermal resistance of DC LEDs to identify parameters that affect the thermal resistance values.

2.1 Basics of LED

An LED is a P-N junction, made out of semiconductor materials, that emits photons when subjected to an external electric field. LEDs are fabricated using GaP (for emissions in red, amber and yellow regions) and GaN (for emissions in near UV, violet, blue and green regions) based compounds. Improvements in internal quantum efficiency, and light extraction efficiency, have enabled the development of high power LED packages [15,16].

The emission wavelength of an LED depends on the band gap of the semiconductor material [17]. The energy of the photon emitted as a result of the radiative recombination, depends on the band gap energy, if the thermal energy is negligible. The band gap in a semiconductor material is the “minimum energy necessary for an electron to transfer from the valence band (E_v) into the conduction band (E_c)” [18]. Figure 1 shows a band diagram of a semiconductor and the direct electron-hole recombination that generates a photon. Direct band gap materials such as GaN, ZnSe & GaAs are preferred over indirect band gap materials such as SiC, Ge, GaP, for high power light emitting devices [19]. This is because efficient radiative recombination occurs in direct band gap materials [20].

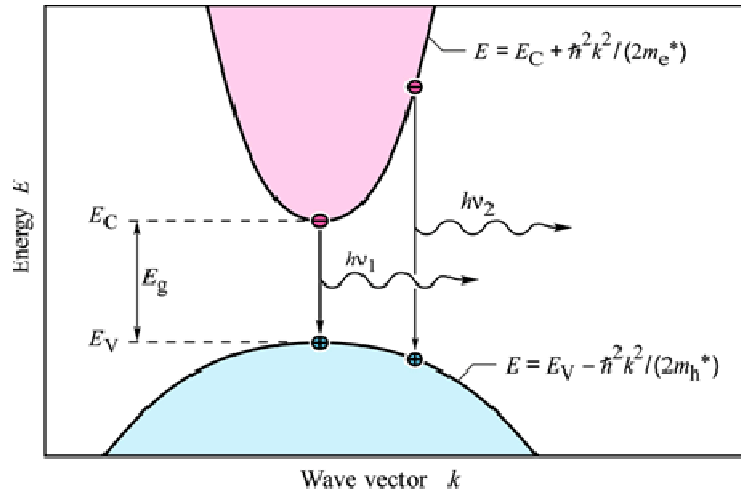


Figure 1: Band gap & electron-hole recombination process [17]

2.2 AC LED package

In recent years, AC LEDs have captured the interest of the LED lighting community. In standard DC LED lighting systems, the AC input from the grid needs to be converted to DC. The loss of power during this AC to DC conversion could range from 10%, to as high as 50%, depending on the quality of the driver [6]. The absence of the AC-DC converter would also higher system reliability, lower cost and smaller form factors in LED luminaires. One limiting factor for AC LED package is, a flickering frequency of 120Hz, which could be uncomfortable for human vision [6].

AC LED packages are fabricated by growing several junctions on an insulated substrate that are connected either in ‘series type’ or ‘bridge type’ configuration. The concept of multi-junction arrays of light emitting diodes, driven at high voltages, has been in existence for a while, but fabrication and reliability challenges have limited the use of this concept in practical applications [21]. The current-voltage characteristic of an AC LED package could be represented as follows [21].

$$V = nV_{diode} + IR \quad 2-A$$

Where,

V– Voltage drop across the package (V)

V_{diode} – Voltage drop across a single diode (V)

n – number of diodes in a string

R – Current limiting series resistance (Ω)

I – Current (A)

According to the above formula, the duty ratio depends on the number of diodes on a string. As indicated in Figure 2, the number of dies in a package is a compromise between the light output and forward voltage of the package.

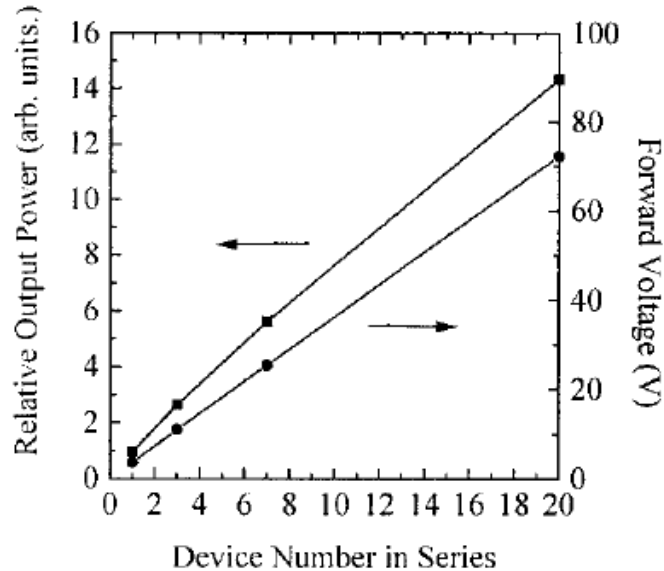


Figure 2: The variation of relative output power and forward voltage with the number of dies in an AC LED package [22]

Tamura et al. [23], developed a packaged LED array, connected in series, on a glass epoxy substrate, that could be driven at 100V (60Hz) AC operating condition. Ao Jing-Ping et al. [22], developed a Indium Gallium Nitride (InGaN) LED series array on a sapphire substrate, as a monolithic package, (Figure 3) that could be directly operated using high AC voltage. Figure 4 shows a series type AC LED package with one string turned on at a time. The series type configuration has a lower active layer utility ratio, since only half of the diodes conduct at each cycle. Yen, et al. [6], developed the Wheatstone bridge configuration (Figure 5) that has a higher active layer utility ratio, because there is a string of dies that always conduct at both AC half cycles.

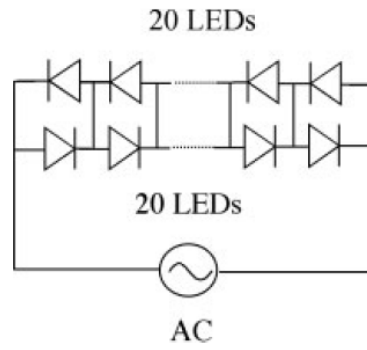


Figure 3: Circuit diagram of a series LED array in an AC LED package [22]

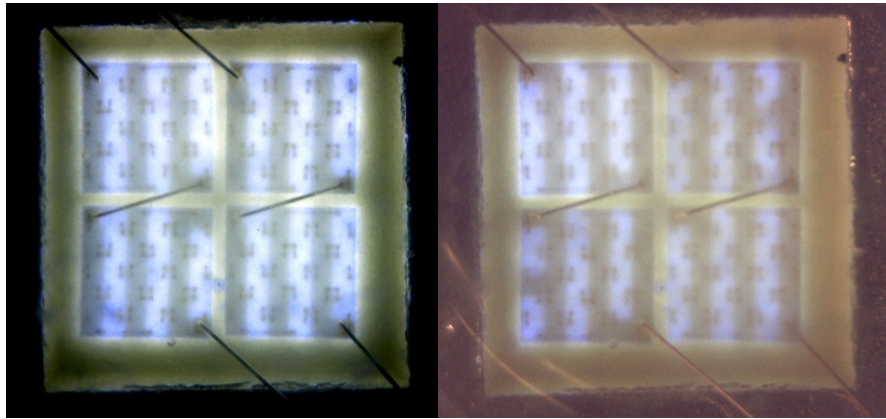


Figure 4: AC LED with series type configuration

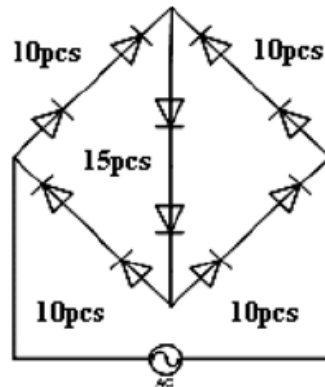


Figure 5: Circuit diagram of the Wheatstone Bridge configuration [6]

2.3 Junction Temperature

Heat generated at the junction is mainly a consequence of non-radiative recombination, extraction inefficiency and ohmic resistance. When electron-hole recombination leads to an emission of a phonon (vibration energy of lattice atoms) it is referred to as a non-radiative recombination [17]. Some factors that contribute towards non-radiative recombination in GaN LEDs are point defects and dislocations in the crystalline structure [24], and Auger recombination [25].

Junction temperature of the diode has a significant influence on its efficiency, reliability and operating characteristics [7]. Temperature also acts as a catalyst for package level reliability issues such as delamination, yellowing of phosphor and lens degradation [7,26,27]. It is therefore critical to know the junction temperature of a device in a given thermal environment. This information is useful for manufacturers of LED packages and lighting fixtures, in order to design efficient and reliable LED lighting systems [28]. System design engineers often want to validate their design by comparing the junction or solder temperature with a prescribed value.

2.4 Measuring Junction Temperature of DC LEDs

Several methods can be found in existing literature to measure junction temperature of DC LEDs. These methods can be broadly categorized into two categories [9,10,11,12,13,14].

1. Electrical test methods
 - Steady state T_j measurement using forward voltage [9,29,14]
 - Transient T_j measurement using transient voltage [10]
2. Optical test methods
 - Direct temperature measurement using nematic liquid crystal thermography [13]
 - T_j measurement using the peak wavelength of the emission spectrum [11]
 - T_j measurement using the relative radiant power distribution in the emission spectrum [12]

The underlying concept behind the above measurement methods are discussed in detail in the following sections.

2.4.1 Electrical test methods

The existing literature discusses several methods that can be used to estimate T_j of a DC LED using forward voltage drop as the temperature sensitive parameter [9,10,14]. The current-voltage relationship of a LED can be expressed using the Shockley equation as follows [30,31],

$$I = I_0 \left(e^{\frac{eV}{nkT}} - 1 \right) \quad 2-B$$

where,

I_0 – reverse saturation current (A)

e – electronic charge (C)

k – Boltzmann’s constant (eV/K)

n – ideality factor

V – forward voltage (V)

T – temperature (K)

The reverse saturation current through a diode is expressed as [30,31],

$$I_0 = I_{ss} e^{\frac{E_a}{kT}} \quad 2-C$$

where,

E_a – activation energy of the semiconductor (eV)

I_{ss} – constant for the device (A)

K – Boltzmann’s constant (eV/K)

T – Temperature (K)

Using equations 2-B and 2-C the following equation can be derived,

$$eV = nkT \ln \left(\frac{I}{I_{ss}} \right) + nE_a \quad 2-D$$

Therefore, it can be proved that there exists a linear relationship between forward voltage and T_j as described above. This relationship can be used to predict the junction temperature of a DC LED. Standardized testing methods for semiconductor devices such

as EIA/JESD51-1 and MIL-STD-750E use this principal to estimate junction temperature [9,29]. The recommended methodology as stated in EIA/JESD51-1 is explained in appendix A.

The forward voltage of the LED needs to be correlated to junction temperature using a calibration factor. The assumption made during calibration is that when the low measurement current or pulsed current is applied, the rise in temperature in junction is negligible and therefore, T_j is equal to the ambient temperature. The reciprocal of the gradient of the calibration curve is referred to as the “K-factor” [9]. The junction temperature of the diode can be estimated using the following formula:

$$\Delta T_j = (V_{FH} - V_{FM}) \times K \quad \text{2-E}$$

$$T_j = T_a + \Delta T_j \quad \text{2-F}$$

where,

ΔT_j – Junction temperature rise under DC steady state operation ($^{\circ}\text{C}$)

T_a – ambient temperature ($^{\circ}\text{C}$)

V_{FH} – forward voltage when heating current is applied (V)

V_{FM} – Forward voltage when measurement current is applied (V)

K – K-factor obtained as explained in appendix A ($\text{V}/^{\circ}\text{C}$).

The EIA/JESD51-1 standard recommends that the calibration should be performed for each specific package [9]. Zong et al. [14], suggested a method, according to the authors, that does not require calibration and is independent from the mounting method, or thermal resistance between the LED and heat sink. This method captures the initial forward voltage of the LED when a DC step (or a sequence of pulses with a short duty ratio) is applied. The initial voltage is recovered by adjusting the temperature of the thermoelectric cooler upon which the LED is mounted. This method is explained in detail in appendix B.

2.4.2 Optical test methods

Peak wavelength shift and centroid wavelength shift of AlInGaP DC LEDs is directly proportional to T_j at different ambient temperatures, and drive currents [11]. The relationship between temperature and peak energy of optical emission can be derived from the Varshni equation [32]:

$$E_g = E_0 - \frac{\alpha T^2}{\beta + T} \quad \text{2-G}$$

Where,

E_g – Band gap energy (eV)

α & β are the Varshni parameters

T – Temperature (K)

The emission spectrum of an InGaN DC LED broadens and its peak wavelength shifts towards short wavelengths, with increasing input current [33,34]. This phenomena can be explained using the quantum confined stark effect that occurs in quantum wells due to piezoelectric field [35], and band filling, that occurs in a local potential minimum of the InGaN well [33]. The quantum confined stark effect is where spatial separation of electron and hole wave functions expands, due to the electric field perpendicular to quantum well walls [36]. This will reduce the band gap, and inter band recombination rate with higher charge densities surrounding the quantum well [37].

A calibration curve that correlates peak emission wavelength with temperature, is obtained by driving the LED with a pulse current which has a small duty ratio, in different controlled temperature environments [11,34]. The junction temperature could be determined by obtaining the peak wavelength shift during steady state operation at a given driving current [11]. The respective formula to convert peak wavelength to junction temperature is given below:

$$\Delta T_j = (\lambda_o - \lambda_{oi}) \times K_\lambda \quad \text{2-H}$$

$$T_j = T_a + \Delta T_j \quad \text{2-I}$$

where,

ΔT_j – junction temperature rise from ambient temperature under DC steady state operation ($^{\circ}\text{C}$)

T_a – ambient temperature ($^{\circ}\text{C}$)

λ_{oi} – Initial turn on wavelength (nm)

λ_o – steady state wavelength (nm)

K_λ – Empirical constant determined using the pulsed current operation of LED in a temperature controlled environment (nm/ $^{\circ}\text{C}$).

Due to some of the reasons mentioned above; instead of using emission peak shift for GaN based white LEDs with YAG Cerium phosphor, the ratio of total radiant energy to radiant energy within the blue emission band was used as the temperature sensitive parameter [12]. At high temperatures the emission spectrum of LEDs gets asymmetrically broadened [38]. Past studies which compared the T_j measured using peak wavelength shift method and forward voltage drop method obtained similar results [39].

2.5 Measuring Junction Temperature of AC LEDs

Thermal parameters of the AC LEDs could be significantly different to that of DC LEDs since the instantaneous input power to the junction of the AC LED varies rapidly within a short period of time. There is limited literature with regard to the thermal properties of AC LEDs. In fact, to date there is no method or standard defined to measure the junction temperature of AC LEDs [3]. It is difficult to directly apply the K-factor theory which is widely used in junction temperature measurement of DC LEDs for AC LEDs, due to the fact that forward bias of AC LEDs vary quickly with time [1].

Even though the instantaneous input power to an AC LED changes rapidly with time, the submount temperature is insensitive to the changes that occur in the junction due to its thermal capacitance [1]. This fact was utilized to correlate the junction temperature with the temperature of the center of the bottom surface of the submount, under DC

operation, using K-factor theory. Junction temperature was measured using the K-factor theory for different levels of DC input power. Based on the experimental results obtained for the DC analysis, the relationship between junction temperature and board temperature was formed.

Since an AC LED package is subjected to an input power that has a frequency of 60Hz, it is plausible that the T_j fluctuates within a range that is determined by the thermal capacitance of the die [1,4]. If power dissipation is expressed in the following form (assuming a sinusoidal function),

$$P_{dissAC}(t) = P_{max} \cdot \sin(\omega t) \quad 2-J$$

Where,

$P_{dissAC}(t)$: AC power dissipation waveform (W)

P_{max} : amplitude of the AC input power waveform (W)

ω : angular frequency (depends on the frequency of AC supply)

Then junction temperature could be expressed as [4],

$$T_{jAC}(t) = T_{jmax} \sin(\omega t - \varphi) \quad 2-K$$

$$T_{jmax} = |Z_{th}(\omega)| \cdot P_{max} \quad 2-L$$

Where,

$T_{jAC}(t)$: Junction temperature waveform

$T_{jmax}(t)$: amplitude of the junction temperature

$Z_{th}(\omega)$: AC thermal impedance (consist of resistive and capacitive components)

φ : phase delay between power and temperature to reflect capacitive nature of thermal impedance.

Hwu et al. [1], predicted the oscillatory behavior of junction temperature using numerical simulation and developed a formula that links the range of oscillation to board temperature. Input power waveform is periodic but not sinusoidal; therefore the harmonic components contribute towards junction heating [40]. If the AC thermal

impedance could be characterized in the frequency domain T_j could be obtained using the following formula:

$$T_{JAC}(t) = \sum_{n=0}^{\pm\infty} Z_{th-n} \cdot P_n \cdot e^{jn\omega_0 t} \quad 2-M$$

Z_{th-n} : Harmonic components of AC thermal impedance

$P_n \cdot e^{jn\omega_0 t}$: Harmonic components of AC input power (Fourier transform of input power)

Poppe, et al. [4], suggested two approaches to obtain the thermal impedance function of the AC LED package. The first method is the use of JEDEC JESD51-1 electrical test method by operating AC LED at high DC voltage. The alternative approach is to obtain the cooling curve of the AC LED when AC input power to the device is disconnected at a given phase angle and use it to obtain AC impedance function .

2.5.1 RMS current recovery method

This method uses the rms value of a current waveform across an AC LED as the temperature sensitive parameter to predict the junction temperature [2]. This method is similar in principal to the voltage recovery method for DC LEDs, which is explained in appendix B.

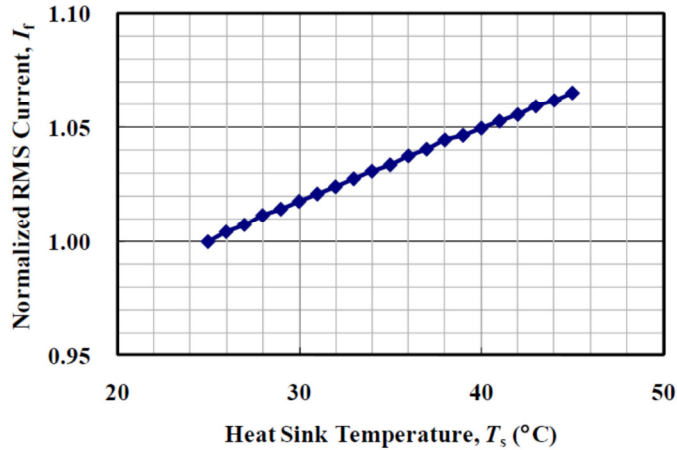


Figure 6: Relationship between first half cycle rms current and heat sink temperature [2]

The LED is operated at a constant AC voltage and is placed in an active heat sink, which is set to a particular temperature level. Initially when the AC LED is at ‘off’ state, it is

assumed that T_j is equal to the cold plate temperature of the heat sink. The input AC voltage is applied at zero phase, and the rms value of the first half cycle of the current is measured. The temperature of the active heat sink is reduced until the rms value of the forward current matches with the rms value of the initial current. When the two forward current values are equal it could be deduced that T_j is equal to its initial value. It was assumed that the first half cycle of the current waveform did not cause a significant heating at the junction.

Zong, et al. [2], stated that within the first AC power cycle, junction temperature increases approximately by 25% of its total rise. Therefore, this method would significantly underestimate the junction temperature.

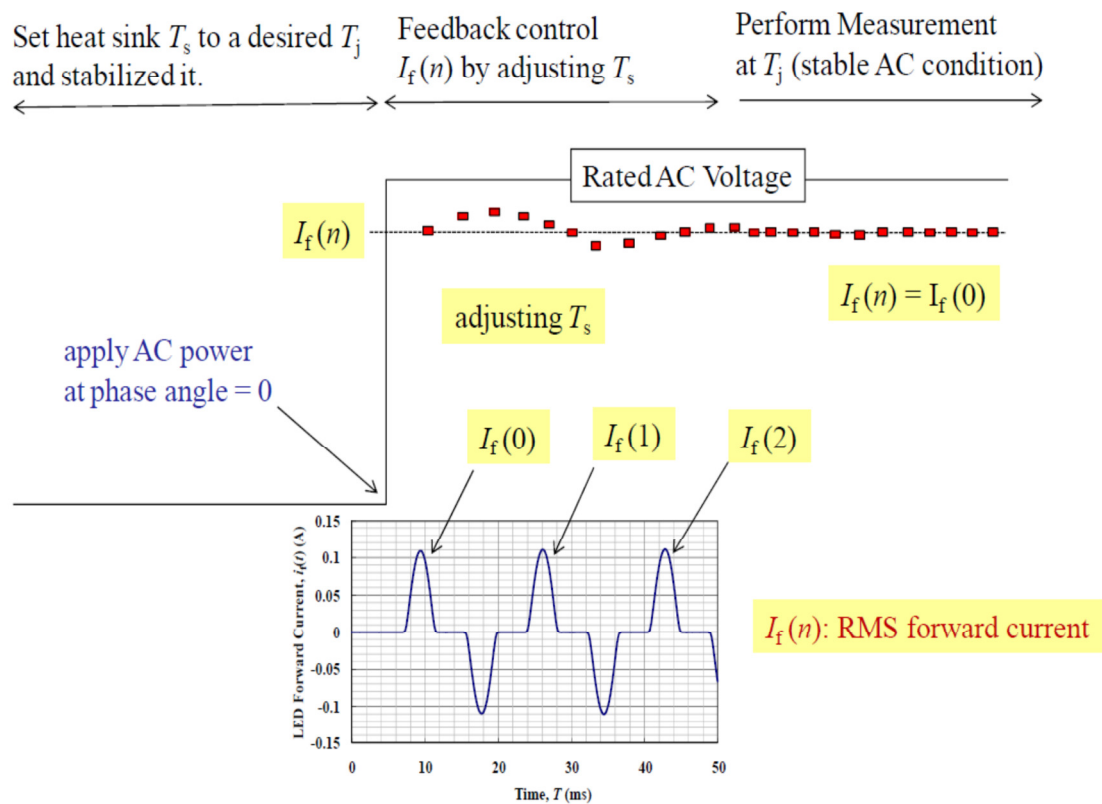


Figure 7: Illustration of rms current recovery method [2]

The past literature on the topic has introduced mathematical models that predict the oscillatory behavior of the junction temperature of an AC LED package [1,4]. Hwu, et al.[1] showed that mean T_j stabilizes at steady state operation. Therefore, it could be inferred that this method attempts to estimate the mean T_j at steady state operation.

2.5.2 Voltage drop method for AC LED

This method uses the voltage drop across the AC LED as the temperature sensitive parameter. A calibration curve is obtained by following the same protocol explained in EIA/JESD51-1 (as explained in appendix A). The input AC current through the package would be zero till the input AC voltage exceeds the forward bias voltage. Therefore, the AC current waveform has a flat zero portion which is referred to as “current dead-zone” hereafter.

The AC LED is driven at its nominal voltage and a small current pulse is applied at the “current dead-zone” of the AC LED, as shown in Figure 8. The voltage drop in the junction, when the pulse is applied, is converted to T_j using the calibration curve. Since the reference current pulse is applied at the dead-zone of the current waveform, the input power to the AC LED is not interrupted. Figure 9 shows that when the reference current pulse is applied at the current dead-zone region, as opposed to at other phase angles, the measured T_j is highest, since the input power to the LED is not interrupted.

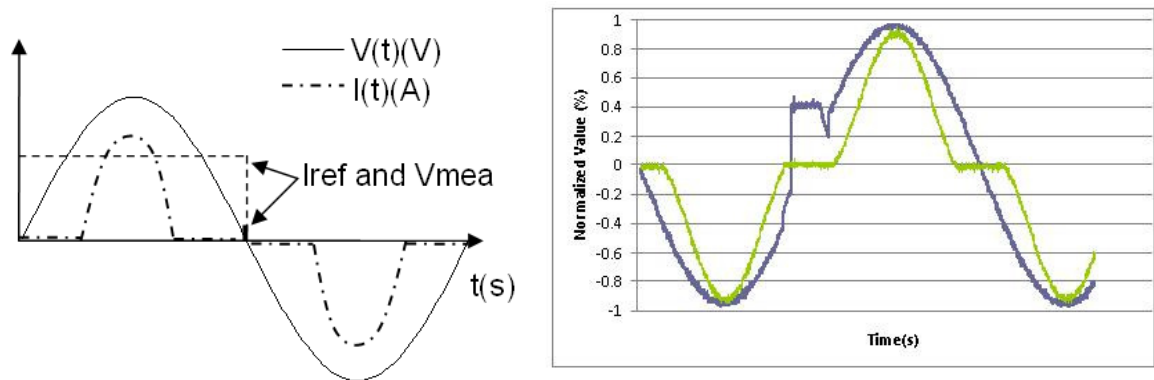


Figure 8: Reference current pulse (I_{ref}) is applied at the current dead-zone region [3]

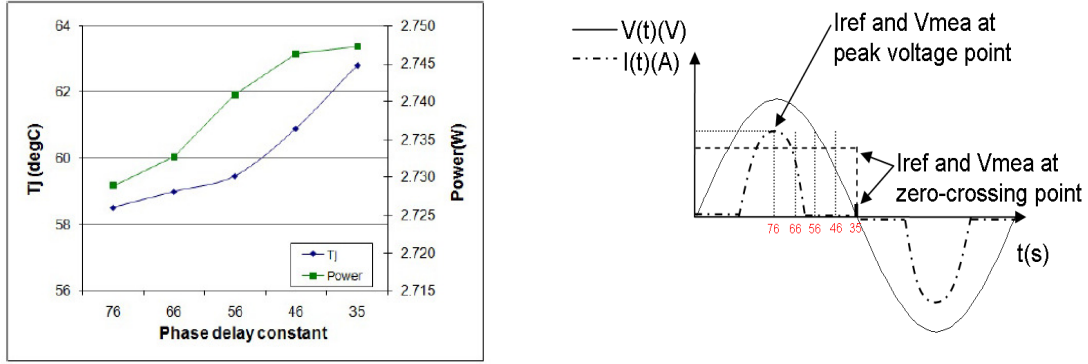


Figure 9: Junction temperature when reference pulse is applied at different phase angles of the voltage waveform [3].

2.6 Thermal resistance

As discussed previously, the junction temperature of a LED cannot be measured directly. It is imperative to know the value of the T_j of a LED installed inside a fixture in order to evaluate the performance of the fixture. The following equation is commonly used for T_j measurement [41].

$$T_j = T_{ref} + R_{thJ-ref} * P \quad 2-N$$

$R_{thJ-ref}$: Thermal resistance between the junction and a reference point ($^{\circ}C/W$).

T_{ref} : Reference point temperature ($^{\circ}C$).

P : Input thermal power (W)

The reference point temperature could be measured using a thermocouple. The measured temperature could be used to predict the junction temperature, using the one dimensional heat transfer formula, 2N. However, for this method to be accurate, a better understanding is required of the thermal resistance between the reference point and the junction. It is important to understand the factors that influence thermal resistance and whether it will remain constant in different application environments.

“The temperature difference between two isothermal surfaces divided by the heat that flows between them is the thermal resistance of the materials enclosed between the two isothermal surfaces and the heat flux tube originating and ending on the thermal

boundaries of the two isothermal surfaces” [42]. According to the formal definition, thermal resistance defined between the junction and a reference point of a LED is correct only if the two surfaces concerned are isothermal and the total heat flux between the two surfaces are known.

Thermal resistance is by rearranging the formula, 2-N [9].

$$\mathbf{R_{thJ-ref} = \frac{(T_j - T_{ref})}{p} \quad 2-O}$$

Instead of using a spatial temperature difference as in 2-O, the temporal difference of the junction temperatures at two different input thermal power conditions can be used to calculate thermal resistance, when the reference point temperature is kept constant [41].

$$\mathbf{R_{thJ-x} = \frac{\Delta T_j(t)}{\Delta P_H} \quad 2-P}$$

Where,

$\Delta T_j(t)$: Difference in the initial and final steady state temperature in the junction ($^{\circ}\text{C}$).

ΔP_H : Difference in the heating power at the junction (W).

According to Poppe et al. [41], the above approach cancels out inaccuracies in junction temperature measurements. The input power used in calculating the thermal resistance should be the thermal power dissipated at the junction. Therefore, the contribution of forward current towards radiative recombination should be considered in calculating thermal resistance [10].

Thermal resistance is defined in the steady state condition. In defining thermal resistance it is implied that heat capacitances between the two isothermal surfaces are fully charged [43]. Therefore at a transient state when the temperature in the package is moving towards the new equilibrium, thermal impedance is defined. Thermal impedance includes the effect of thermal capacitance. Poppe, et al. [40], defined the “effective AC thermal impedance” as,

$$Z_{\text{thAC}} = \frac{\Delta T_j}{P_{\text{dissAC-mean}}} \quad 2\text{-Q}$$

Where,

Z_{thAC} : effective AC thermal impedance

ΔT_j : maximum T_j change when AC power is switched-off at a particular phase angle

$P_{\text{dissAC-mean}}$: mean thermal power dissipation

2.7 Characterization of thermal resistance of DC LED packages

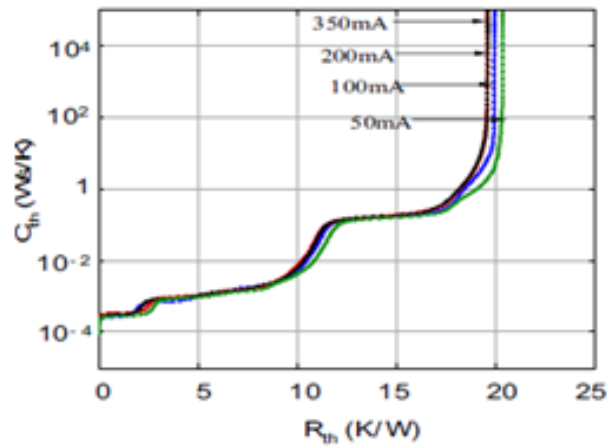
Manufacturers specify the thermal resistance of their packages as a series of thermal resistances from junction to the ambient [44]. The assumptions being that the heat flows in a one dimensional path and thermal resistance is local to a particular part of the package (ex: from junction to heat slug). Therefore it does not depend on the thermal conductivity or convective heat transfer coefficient of the overall thermal path [45]. The heat spreading in the board makes it impossible to separate between conduction and convection heat transfer when measuring thermal resistance. Therefore, the measured thermal resistance between the junction and the board depends on the application environment [9,29]. Past research on the topic also provide evidence that shows measured thermal resistance changes with input power [10,46,47,48,49] .

Jayasinghe et al. [47], showed that electrical input power, ambient temperature, amount of heat sink and heat sink orientation all have an impact on the thermal resistance. Past studies indicate that when the ambient temperature was raised, the measured thermal resistance of the DC LED package increased [47,49].

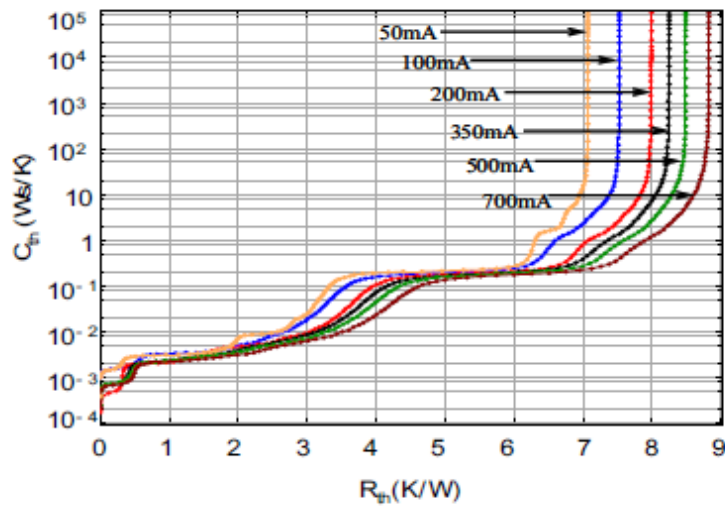
There is evidence of both an increasing and decreasing trend of thermal resistance with input power, for DC LED packages [10,46,48,49]. The effects of input current on the thermal resistance of a DC LED package depends on the ratio of internal and external series electric resistance [46]. The LED could be represented as a model with an ideal diode with an internal and, external electrical resistances connected in series. If the external package resistance is significantly larger than the internal resistance of the

diode, then the thermal resistance would decrease with input power. Figure 10 shows the results of a study that measured the thermal resistance from junction to case, of 1W and 5W LED packages at different driving currents.

The thermal resistance could vary with input power due to; decreasing quantum efficiency at high temperatures, degeneration of materials in a LED package and conductivity changes of GaN and thermal interface materials [47,49].



(a)



(b)

Figure 10: Variation of thermal resistance with input power for 1W (a) and 5W (b) DC LED [46]

The thermal resistance of multichip GaN LED packages is lower than the thermal resistance of single chip GaN LED packages [50]. The thermal resistance from junction to heat slug decreases proportionally with the number of chips in the package. This phenomenon occurs due to an increase in the heat flow area with the higher number of chips in the package.

2.8 Summary of the literature review

Several methods have been suggested to measure the junction temperature of a DC LED. Among these methods, the forward voltage drop method (refer to appendix A) is widely used in the industry to measure the junction temperature of DC LEDs [9]. The forward voltage recovery method (refer to appendix B) is being suggested as an alternative. The forward voltage recovery method yields a similar thermal resistance measurement as the forward voltage drop method used by the industry [14].

There are no existing standards to measure the thermal resistance of an AC LED. One suggested method is to measure the junction temperature by recovering the initial half cycle rms current [2]. An alternative method proposed is to apply a reference current pulse at the dead-zone of the current waveform of an AC LED and measure the voltage drop at that instance [3]. The latter method uses a calibration curve, derived by heating the LED to a known temperature, T_1 and measuring the voltage by applying a small reference DC current. The thermal resistance measurements obtained using the voltage drop method for AC LEDs, was significantly higher than the thermal resistance values obtained through rms current recovery method using an active heat sink [3]. The same study identified that the first half cycle heating in the junction, in the rms current recovery method using active heat sinks, could be the possible discrepancy for this difference. An objective of this thesis is to investigate the reasons for this difference in thermal resistance values measured using two different methods.

Thermal resistance of a DC LED changes with input power [10,46,47,48,49]. The direction of variation in the thermal resistance with input power depends on the ratio

between the internal and external resistance of the package [46]. If the external resistance of the package is significantly higher than the internal resistance, then the thermal resistance of the package decreases with input power. The thermal resistance of DC LEDs increase with ambient temperature [47,49]. This is explained using the heat spreading phenomenon that occurs in the board of the LED, which makes it impossible to separate thermal resistance due to conduction and convection [45].

No similar analysis exists on the behavior of thermal resistance of AC LED packages at different input power and ambient temperature conditions. Therefore this thesis studied the behavior of the thermal resistance of AC LED packages with increasing input power and ambient temperature.

3. Hypotheses

Four hypotheses were developed based on the literature review.

3.1 Hypothesis 1

Thermal resistance of an AC LED measured using voltage drop method for AC LED and, rms current recovery method after adjusting for first half cycle heating in the junction will agree within 10%.

A previous study showed that there is approximately a 50% difference in the thermal resistance values measured using the two methods. Researchers hypothesized that the reason for such a significant difference is the first half cycle current heating in the junction which is not accounted for in rms current recovery method [3]. The thesis would quantify the heating in the junction during the first half cycle of the current waveform and compare the results after adjusting for this initial heating.

A pilot study was performed to understand the uncertainties of the two measurement setups. The details of the pilot study are given in appendix C. The pilot study revealed that the measurement uncertainty in the experiment set up for rms current recovery method is 10%. Therefore, it was hypothesized for the group of LEDs tested, that both methods should agree within 10%.

3.2 Hypothesis 2

For AlInGaP ACLED package;

If the junction temperature (Junction temperature is estimated using voltage drop method) increases then the peak wavelength will shift to longer wavelength, and the rate of peak wavelength shift with temperature will be linear.

The above hypothesis is based on past literature that explained peak wavelength of an AlInGaP package is strongly dependent on the junction temperature [11,34].

3.3 Hypothesis 3

In the range of 25⁰C to 75⁰C

If the ambient temperature surrounding the AC LED increases then the thermal resistance value will increase.

The above hypothesis is developed based on the previous studies done for DC LEDs [47,49]. This phenomenon was explained using the heat spreading that occurs in the board, which makes the measured thermal resistance dependent on the convective heat transfer coefficient [45]. Since same phenomenon is valid for AC LED packages, it was hypothesized that it should also show a similar trend as DC LEDs.

3.4 Hypothesis 4

In the range of 110V-130V,

If the input voltage to the AC LED increases then the thermal resistance value will decrease.

The above hypothesis was developed based on previous studies done for DC LEDs [10,46,47,49]. Literature states that the direction of change of thermal resistance with input power depends on the ratio of internal/external resistance of the LED package. If the external series resistance is greater than the internal resistance of the package, then

the thermal resistance will decrease with input power [46]. AC LED packages have a substantial external series resistance to balance voltages in the two reverse parallel strings of diodes, therefore it is a reasonable hypothesis based on the literature for DC LEDs that with increasing input power the thermal resistance value for AC LEDs would decrease.

4. Experiment

4.1 Hypothesis 1: Comparison of measurement methods

The goal of the hypothesis 1 is to compare the thermal resistance values measured using the voltage drop method and rms current recover method after adjusting for first half cycle heating.

4.1.1 Experiment Variables

4.1.1.1 Independent variables

➤ Thermal resistance measurement methods for AC LED

The voltage drop method for AC LED [3]

The rms current recovery method [2]

➤ Cold plate temperature of the thermoelectric cooler

Temperature settings were chosen so that the pin temperatures of the package are close as possible at the instance where the junction temperature was measured in both methods. Exact matching of pin temperatures are not possible due to different approaches adopted in the two measurement methods. Temperature settings of 35⁰C, 55⁰C & 60⁰C were selected for voltage drop method. An initial temperature setting of 50⁰C, 70⁰C & 75⁰C was selected for the rms current recovery method.

* Portions of this chapter previously appeared as: A. Jayawardena, Y.-W. Liu, and N. Narendran, "Methods for estimating junction temperature of AC LEDs," in *Proc. SPIE*, vol. 8123, San Diego, CA, 2011, pp. 81230I-1-81230I-6, doi:10.1117/12.904056.

4.1.1.2 Dependent variables

➤ The sense voltage

Voltage measured when the reference current is applied at the current dead-zone during synchronized AC operation of the AC LED.

➤ The rms value of the current through AC LED

The rms value of the initial half cycle of the AC current waveform applied across the LED

4.1.1.3 Extraneous variables

➤ Thermal mass

Identical heat sink was used for both methods to maintain identical thermal mass. Literature revealed that heat sink mass influence thermal resistance, as its influences the heat transfer coefficient from device to ambient [47].

➤ Mounting orientation

The mounting orientation of the LED affect thermal resistance since it affects the heat transfer coefficient from device to ambient [47]. The device under test was mounted vertically in both cases.

➤ Cooling method

Junction to case thermal resistance depends on the cooling method employed during the testing [43]. Active cooling was employed in order to maintain as similar a thermal flux environment as possible around the junction for both methods.

➤ Thermal bonding to the heat sink

The device was attached to the active heat sink mechanically using screws.

➤ Lead wire resistance

Identical length of lead wires and, identical connectors were employed for both methods.

➤ Air flow

Air flow velocity influences the heat transfer coefficient as it affects natural convection. In order to minimize the influence of varying air flow velocities on the thermal resistance measurement, the LED was covered using an enclosure.

➤ Measuring instruments

The same measuring instruments were employed wherever possible in order to ensure uniform impedances in the circuit, and to minimize measurement errors related to measuring instruments.

4.1.2 Experiment set up: voltage drop method for AC LED

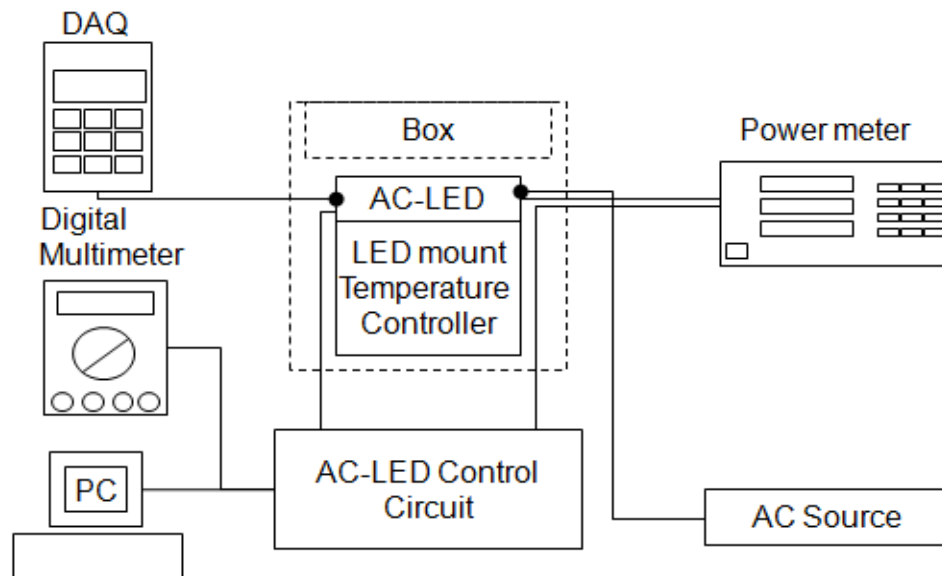


Figure 11: Experiment set up for voltage drop method [3]

A thermoelectric cooler (Arroyo Instruments) that uses the Peltier effect was used to mount the AC LED. The thermistor (10k Ω) senses the temperature of the surface that is in contact with the board of the AC LED. The temperature controller uses feedback control to set the heat sink surface at the required temperature.

The AC LED was enclosed to minimize the interference of air flow on the measurements. The room temperature was not regulated during the experiment. A data acquisition unit (Agilent 34970A) was used to acquire temperature measurements of the J-type thermocouple attached to the AC LED pin. The 24 hour accuracy of the temperature measurement of the data acquisition unit with a J-type thermocouple is $\pm 1^{\circ}\text{C}$ [51].

The AC LED control circuit was custom built for this experiment to perform following functions. Refer appendix D for details on the functionality of the control circuit and its implementation.

- Supply the AC LED with a DC calibration current and sample and hold the voltage across the AC LED at this calibration current.
- Insert the reference current pulse at the desired phase angle of the AC current waveform.
- The control circuit also has the ability to apply the input AC voltage waveform to the LED starting from any specified phase delay.

AC power supply (California Instrument; Model 1001P) with a load voltage regulation of $\pm 1\%$, frequency tolerance of $\pm 0.02\%$, output noise level of $< 0.1\text{V}$ and harmonic distortion of $< 0.55\%$ was used to provide a stable AC power supply to the AC LED.

A digital multimeter (Agilent 34401A) was used to read the voltage measurement sampled and held by the SMP04ES amplifier. The accuracy of the voltage reading of the digital multimeter in the 10V (this was the range used by the circuit) range is $\pm 0.175\text{mV}$ [52].

A power meter (Yokogawa WT210) was used to measure electrical input power to the AC LED. The power measurement has a basic accuracy of $\pm 1\%$ [53]. The power measurement was performed separately from the voltage measurements in order to ensure that the internal resistance and capacitance of the power meter doesn't interfere with the voltage measurements.

4.1.3 Experiment procedure: voltage drop method for AC LED

In order to determine a suitable calibration current the voltage-current characteristics of the AC LED was obtained using a source measurement unit (Yokogawa GS610). The AC LED was attached to a thermoelectric cooler that has a temperature setting of 25°C. A DC voltage sweep from +110V to -110V with 100mV increments were performed.

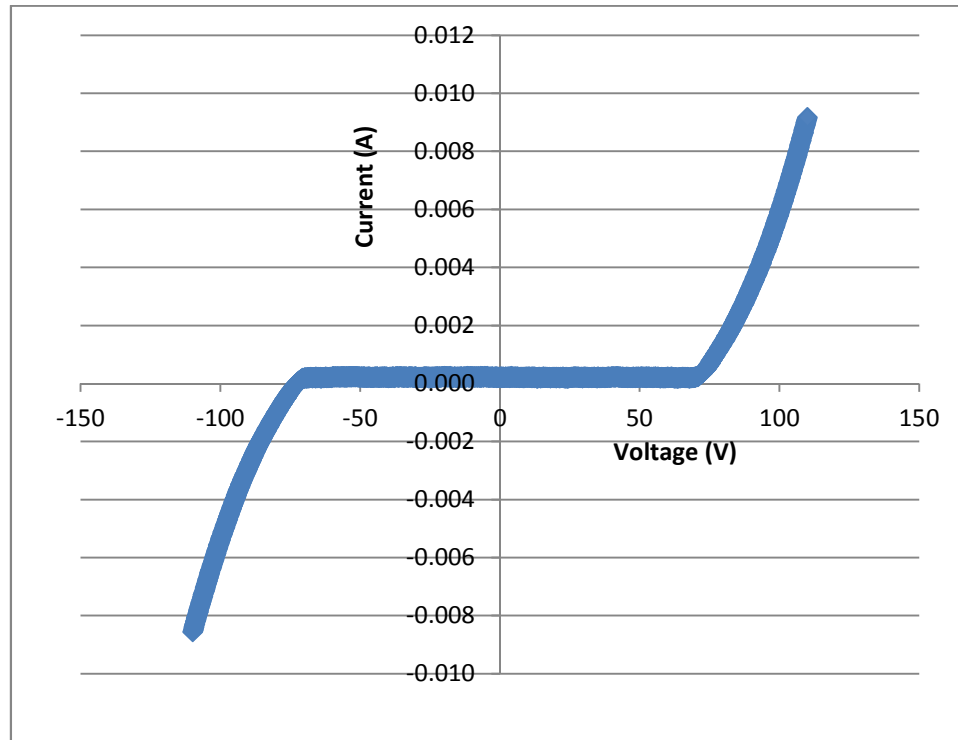


Figure 12: Voltage-current characteristics of a white AC LED

The calibration current was determined using the current-voltage characteristics of the sample shown in Figure 12. Following factors were considered in choosing the calibration current.

- The calibration current should fully forward biased the LED
- It should not lead to significant resistive heating in the junction

The calibration current was determined to be 0.06 mA based on above considerations.

A J- type thermocouple is attached to the center of the submount of the AC LED package. The center of the submount of the package is defined as the reference point at temperature at this point is referred to as the pin temperature here after in the thesis. The J-type thermocouples that comply with IEC584-2 have a standard error of 1.5°C [54].

The thermocouple was attached using the thermal epoxy. The AC LED package was attached to the thermoelectric cooler using mechanical screws. Screws were tightened so that a uniform pressure is applied to ensure proper contact with the metal core printed circuit board (MCPCB) and the surface of the thermo electric cooler to avoid air gaps.

The calibration current was applied and voltage across the AC LED was measured by adjusting the temperature of the active heat sink in 5⁰C steps from 25⁰C to 75⁰C. It was assumed that at calibration current the pin temperature of the AC LED is equal to junction temperature. All voltage readings were obtained after pin temperature reached thermal stability. The criterion for thermal stability is that the variation of five pin temperature samples obtained at every one minute interval is less than 0.1⁰C. This thermal stability criterion was defined based on the guidelines specified for voltage drop method for DC LEDs. The calibration curve in Figure 13 of a GaN AC LED sample shows a strong linear correlation between forward voltage and pin temperature.

Voltage measurements at eleven different points were obtained to check the linearity of the LED. The linear relationship between voltage and T_j is a prerequisite to use voltage drop method for AC LED. Further, the eleven point calibration will also improve the accuracy of the T_j measurement. The calibration curves for both strings of LEDs in the AC LED package were obtained to verify whether they are substantially different. There were no substantial differences between the calibration curves obtained for the two strings of LEDs.

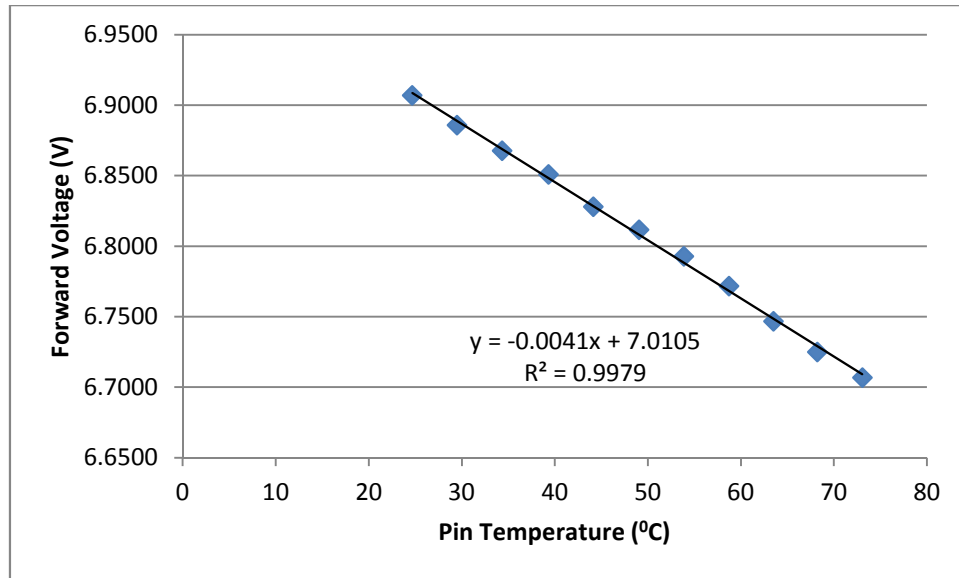


Figure 13: Calibration curve for white AC LED

A reference current pulse was applied at the current dead-zone region of the AC LED when it is in AC operation as shown in Figure 14. The reference current pulse is of the same magnitude as the calibration current. The width of the current pulse was 3ms. Voltage across the AC LED when this pulse is applied is measured after a fixed measurement delay (1ms) upon start of the pulse to avoid switching noise in the signal. Application of the pulse at the current dead zone ensures that input power to the AC LED is not interrupted.

When the pin temperature of the AC LED reached the thermal stability criterion, the forward voltage was measured by applying the reference current pulse at the current dead-zone. The voltage measurements obtained by applying the reference current during the AC operation of the LED was converted to junction temperature using the calibration curve. This value corresponds to the average junction temperature of all junctions in the AC LED package. The pin temperature readings obtained at every 1 min interval using a data acquisition unit was stored in the computer to calculate thermal resistance of the package.

Input electric power to the LED was measured separately from the voltage measurement to avoid the requirement of connecting a power meter between the AC LED and the control circuit. It was observed that the connection of a power meter between the AC LED and the control circuit influences the calibration due to its internal impedance. The input electric power was measured under same operating conditions and upon pin temperature meeting the thermal stability criterion defined above.

Optical power of the AC LED package was measured using an eight inch integrating sphere set-up. The details of the optical power measurement set up and the calibration procedure is explained in detail in appendix E.

At each temperature setting three independent readings were obtained at random order, to determine the measurement uncertainty. Electrical input power and optical power was also measured at each temperature setting.

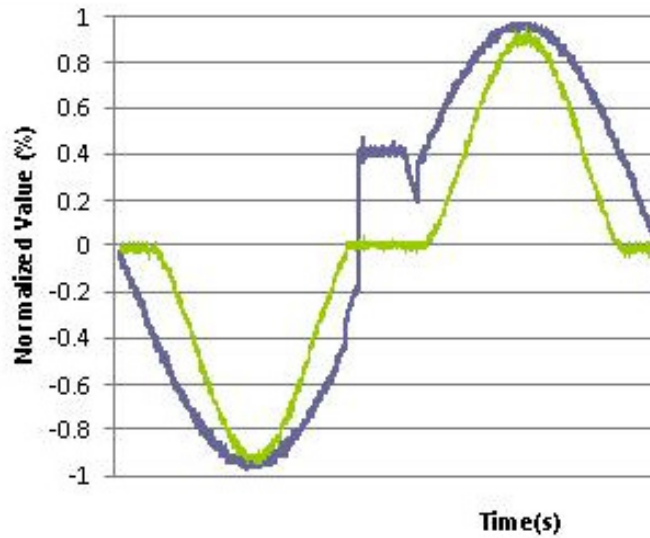


Figure 14: Reference current pulse at the current dead-zone of the AC LED

4.1.4 Experiment set up: rms current recovery method

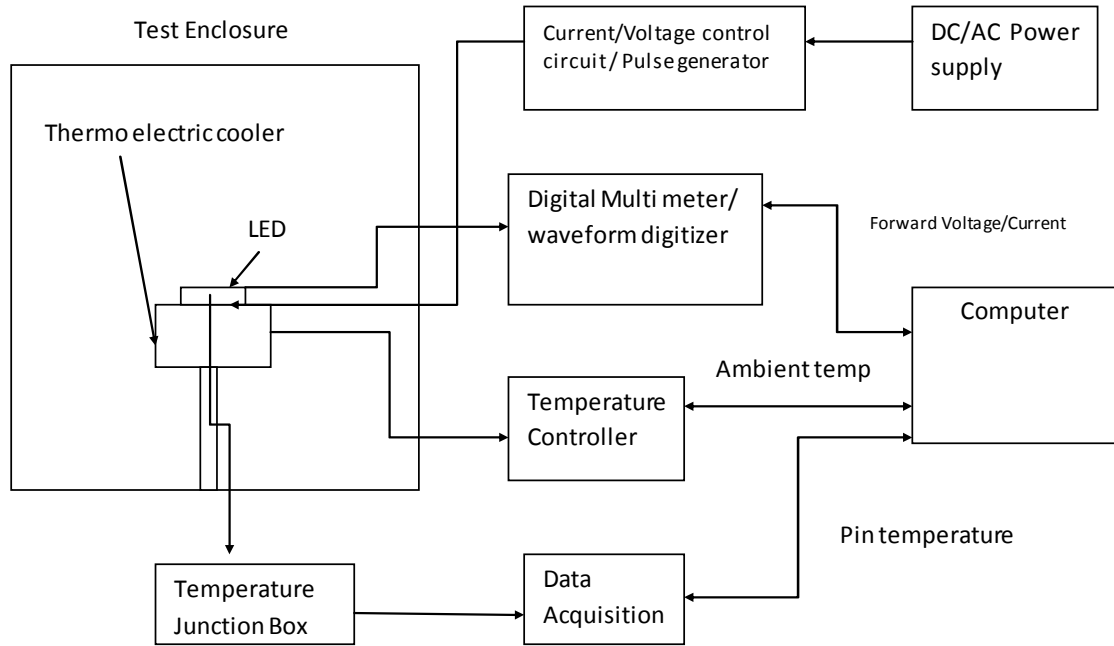


Figure 15: Schematic diagram of the experiment setup for rms current recovery method

The identical thermoelectric cooler described in 4.1.2 was used for this study. The pin temperature of the AC LED was acquired using a data acquisition unit along with a J-type thermocouple. The control circuit monitors the input AC voltage waveform generated by the AC power supply (California Instrument 1001P), and applies the AC voltage from the zero phase angle. The control circuit at the same instance would generate a trigger input to the waveform digitizer (National Instruments PCI-6143) to initiate a scan. The waveform digitizer would measure the current waveform by measuring the voltage across a precision resistor (249Ω , 0.1%, $5\text{ppm}/^\circ\text{C}$ & 0.25W) that is in series with the AC LED.

The waveform digitizer has a sampling speed of 250ks/s with a 16 bit resolution. The sampling rate was chosen considering the fundamental frequency of the AC input waveform, and total harmonic distortion in the output current waveform of the AC power supply. The 16 bit resolution was deemed important since the sensitivity of the current to a 1°C change in T_j of an AC LED is in μA range. The digitized current

waveform was acquired and analyzed using LabView 2009 software to calculate first half cycle rms current.

The experiment setup managed to replicate the first half cycle rms current vs. temperature relationship demonstrated by Zong, et.al [2], in their experiment with statistically significant ($P < 0.05$) correlation.

4.1.5 Experiment procedure: rms current recovery method

An AC LED with a J-type thermocouple attached at the center of the submount (reference point) using thermal epoxy was attached to the thermoelectric cooler. The reference point temperature is here after referred to as the pin temperature in this thesis. The AC LED was attached to the thermoelectric cooler using mechanical screws. The AC LED package was initially heated to a predetermined temperature and was allowed to thermally stabilize. The same thermal stability criterion as described in 4.1.3 was used in this set up. It was assumed initially the T_j is equal to the pin temperature of the AC LED.

The AC voltage was applied from the zero phase angle and the first half cycle rms current was measured. Then the temperature setting of the thermoelectric cooler was adjusted till the measured rms current at steady state, is equal to the first half cycle rms current. The steady state rms current measurements were obtained using the same waveform digitizer at every 1s interval. The temperature was adjusted in 1°C steps since the minimum resolvable pin temperature measurement using a J-type thermocouple was 1.5°C . The temperature at which the measured rms current that is closest to the initial half cycle current within 1°C tolerance was considered as the recovered pin temperature. At this point, the junction temperature is equal to the pin temperature of the package that was measured just before AC measurements. Thermal resistance can now be calculated as,

$$R_{\theta J-p} = \frac{(\text{Initial Pin Temperature} - \text{recovered pin temperature})}{(P_{\text{electrical}} - P_{\text{optical}})}$$

The optical power was measured as explained in appendix E, at the recovered pin temperature. The electrical input power was also measured at the same recovered pin temperature using a watt meter.

4.1.6 Experiment procedure: the first half cycle heating

The thesis quantify the temperature rise in the first half cycle of the AC current waveform. The thermal resistance of the AC LED package measured using rms current recovery method was recalculated with this new information. When the initial half cycle rms current is recovered,

T_j of the AC LED package = T_j of the package just after the first half cycle of current

Therefore thermal resistance equation can be re-written as,

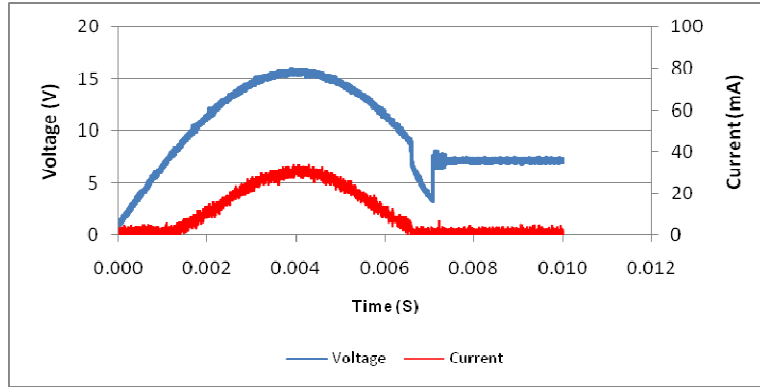
$$R_{\theta J - P} = ((Initial\ Pin\ Temperature + Temperature\ rise\ in\ first\ half\ cycle - recovered\ pin\ temperature) / ((P_{electrical} - P_{Optical})))$$

The heating profile of the AC LED during the first half cycle of the AC current was obtained, by inserting the reference current pulse at different phase angles of the AC input voltage waveform. The forward voltage drop of the AC LED package was measured at the instance the reference current pulse is applied. The Figure 16 illustrates the input AC voltage and current waveforms when the reference current pulse is inserted at different phase angles. The insertion point of the reference current pulse was shifted every 0.6ms intervals. The control circuit explained in appendix D was used for this purpose. The calibration curve obtained as explained in 4.1.2 was used to convert measured voltage to T_j .

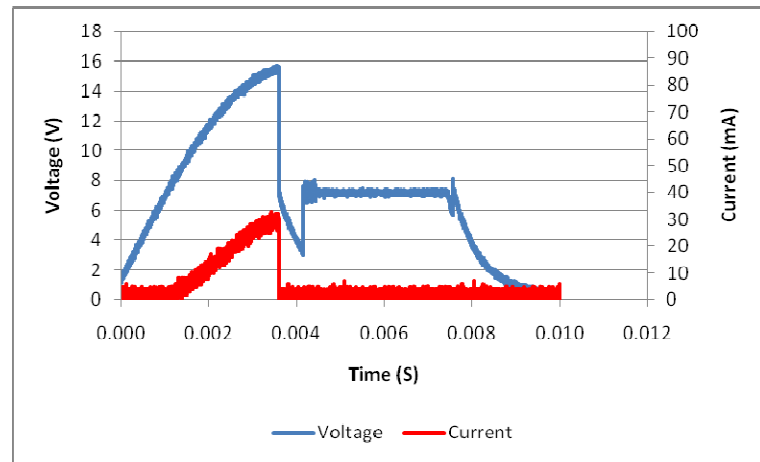
The T_j measured is not the instantaneous temperature of the junction but the temperature rise in the string of junctions due to total thermal power dissipated in the junction. The measured junction temperature represents the average temperature rise in all junctions in a string, of the AC LED package. For example the measured temperature rise in junction when reference current pulse is applied as shown in Figure 16 (a) is due to total input

power applied during the first half cycle of current waveform. Whereas the measured junction temperature rise when reference current pulse is applied as in Figure 16 (b) is due to the integrated input power up to the time where reference pulse is applied. The measured junction temperature in Figure 16 (c) should be equal to pin temperature since at the point of measurement LED had not reached their forward bias voltage.

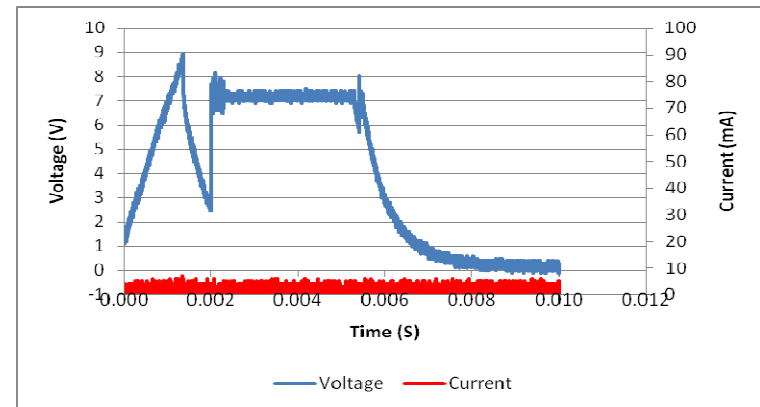
The AC LED package was attached to the thermoelectric cooler during the measurement. The temperature rise during the first half cycle of the AC current waveform was measured at numerous temperature settings (25⁰C, 50⁰C & 75⁰C). Three repeated measurements were obtained at each temperature setting to determine the uncertainty of the measured values. The input AC power was supplied using an AC power supply (California Instruments model 1001P).



(a)



(b)



(c)

Figure 16: The reference current pulse at different phase angles of the first half cycle of AC voltage waveform

(a) Immediately after the first half cycle of current (b) At the half way point of the current & (c) Just before the string of LEDs become forward biased

In Figure 17 junction temperature remains at the ambient temperature till the string of LEDs become forward biased. Junction temperature increases rapidly during the first half cycle of current waveform. When the AC voltage dropped below the threshold the string of LEDs is no longer forward biased, hence the junctions will cool down as revealed in Figure 17. However the thermal capacity of the AC LED package ensures that the junction will not cool down to its initial value when the current across the string of LEDs become zero. Three repeated measurements were obtained at different temperature settings of the thermoelectric cooler to determine the uncertainty of the junction temperature measurements.

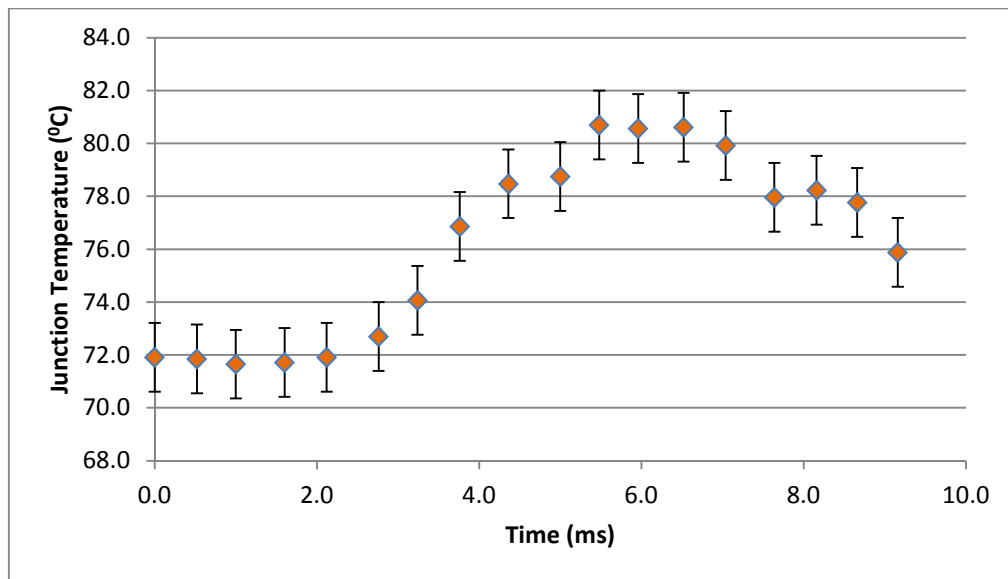


Figure 17: Heating profile of the string of junctions of an AC LED package at 120V at 75⁰C during the first half cycle of the AC voltage waveform

4.2 Hypothesis 2: peak wavelength shift method

Peak wavelength shift of the AC LED package was correlated with junction temperature that was estimated using voltage drop method.

4.2.1 Experiment variables

4.2.1.1 Independent variables

- Cold plate temperature of the thermoelectric cooler
- Input voltage

Input AC voltages (rms) of 110V, 120V & 130 V were used during the experiment.

4.2.1.2 Dependent variable

- Spectral power distribution (SPD) of the AC LED

The SPD was used to calculate the peak wavelength of the device under test at different cold plate temperatures and input power conditions. Peak wavelength was calculated using the spline interpolation function in MATLAB.

4.2.1.3 Extraneous variables

- Ambient light

The measurement was performed in the Robert E. Levin photometry lab with ambient light switched off. A spectroradiometer was placed as close as possible to the integrating sphere, so that it is capable of producing a strong enough output signal when the AC LED is running at calibration current.

- Thermal stability of the AC LED

All spectral power distributions were obtained after the pin temperature of the LED reached the temperature stability criteria defined prior to the experiment. The device reached the thermal stability, when the variation in pin temperature measured over a 5 minute period at every 1 minute interval is less than 0.1°C .

➤ Chromatic distribution

Instead of pointing the spectroradiometer directly at the source it was pointed to the white reflective surface of an integrating sphere.

4.2.2 Experiment procedure: peak wavelength shift method

A GaP based AC LED package with four high voltage chips was used for this study. A J-type thermocouple was attached to the center of the submount of the package to measure pin temperature. The J-type thermocouple connected to the data acquisition unit measured the pin temperature of the package. The package was attached to the thermoelectric cooler using mechanical screws. The AC input power to the package was provided through a control circuit (explained in appendix D). The control circuit receives its regulated AC input from an AC power supply (California Instruments 1001P). The LED mounted on the thermoelectric cooler is emitting light in to an 8 inch integrating sphere through a port. A spectroradiometer, PR705 with a wavelength range of 380nm to 780nm and a spectral accuracy of $\pm 2\text{nm}$ is looking in to the integrating sphere through a port to obtain the spectral power distribution of the emission.

The first step of the experiment was to identify a suitable calibration current to obtain a calibration curve. The calibration current was determined after considering the factors explained in 4.1.3. In addition the magnitude of the calibration current is constrained by the sensitivity of the spectroradiometer. In order to identify the appropriate calibration current peak wavelength at different input currents were measured.

A source measurement unit (Yokogawa GS610) was used to provide a range of DC input currents (20mA, 15mA, 10mA, 5mA, 1mA, 0.1mA, 0.01mA) to the AC LED package. The temperature of the thermoelectric cooler was set at 25°C . The spectral measurements were obtained when LED reached thermal stability (as described in 4.2.1.3). The cubic spline interpolation function in MATLAB was used to identify the peak wavelength value of the spectrum. The measurements were performed at three different temperature settings (25°C , 50°C & 75°C). The results obtained are shown in Figure 18.

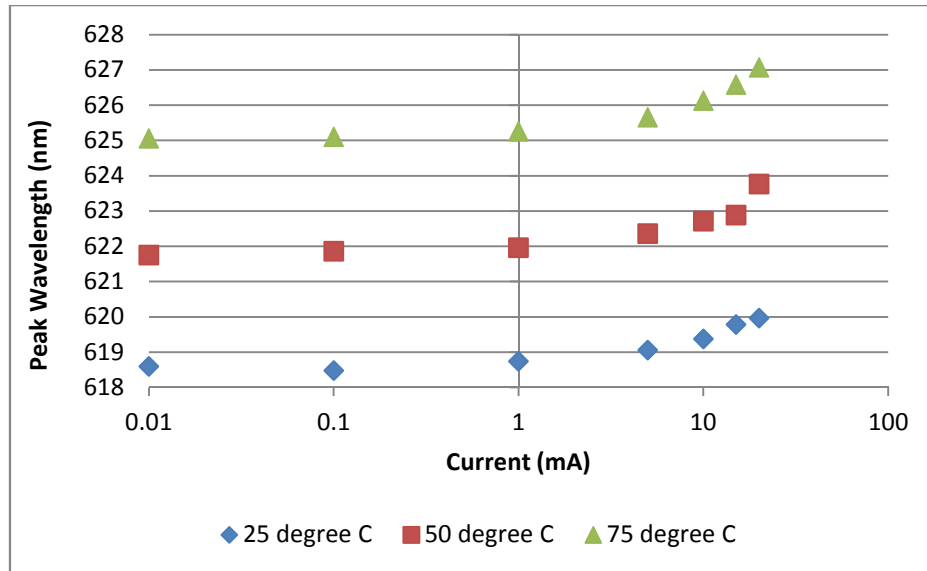


Figure 18: Variation of Peak Wavelength with DC current of a GaP based AC LED package

According to the data plotted in Figure 18, it is clear that when the driving current is less than 0.1mA there is no substantial shift in the peak wavelength. The repeated measurements showed that the measurement uncertainty of peak wavelength is $\pm 0.25\text{nm}$, when cubic spline interpolation was used to find the peak wavelength value of the measured spectrum.

Based on the above analysis a DC reference current of 0.06mA was chosen to obtain the calibration curve. The minimum DC current pulse the voltage drop circuit could produce with least noise is 0.06mA. The use of identical calibration currents in both experiment set ups has the advantage of maintaining similar measurement conditions. The calibration curve was obtained by measuring the emission spectrum from 25⁰C to 75⁰C at every 5⁰C temperature intervals.

After obtaining the calibration curve the spectral power distribution of the LED was measured at three AC input voltage conditions (110V, 120V & 130V). At each input voltage condition, spectral power distribution was obtained at three temperature settings (25⁰C, 50⁰C & 75⁰C). All readings were obtained after the AC LED reached thermal stability criterion.

Hypothesis 3: variation of thermal resistance with ambient temperature

The hypothesis verifies, whether the thermal resistance of AC LED packages increase with ambient temperature range of 25⁰C to 75⁰C.

4.2.3 Experiment variables

4.2.3.1 Independent variables

➤ Cold plate temperature

The ambient temperature surrounding the LED was varied using the thermoelectric cooler/heater. Cold plate temperature was adjusted to 25⁰C, 50⁰C and 75⁰C. The temperature range was selected considering the typical ambient temperatures in the operating environment of AC LED packages. The upper limit of the cold plate temperature is limited to 80⁰C.

4.2.3.2 Dependent variable

➤ The sense voltage

This is the voltage across the junction when the reference current pulse is applied at the dead-zone of the current waveform in the voltage drop method for AC LED. This is the temperature sensitive parameter that is used to predict the junction temperature.

4.2.3.3 Extraneous variables

➤ Electrical input power to the junction

Electrical input power to the junction influence the thermal resistance of the DC LED [46,48,49]. According to literature increasing the ambient temperature and increasing input power has opposing effects on the thermal resistance [49]. In order to minimize the effect of changing input electric power on thermal resistance, the input voltage was kept constant; hence the order of magnitude change of input electric power is small. Even though the AC LED is operated at a constant AC voltage, since the current increase with the operating temperature input power to the AC LED would be different at different temperature settings. Input power to the LED is measured when AC LED becomes thermally stable.

➤ Optical power

The conversion efficiency of input electric power to optical power changes with ambient temperature. In order to account for this, optical power of the LED is measured in an integrating sphere at the respective cold plate temperature as explained in appendix E.

➤ Air flow velocity

The AC LED was enclosed so that changes in the air flow velocity during the experiment have a minimum effect on the thermal resistance measurement. Changes in the air flow velocity influence the natural convection and thereby change the heat flux environment surrounding the junction. The use of active cooling further minimize the influence of air flow rate surrounding the LED because instead of having multiple heat flow paths, there is a single dominant heat flow path regulated by the active cooling device.

4.2.4 Experiment procedure

Two GaN based white LED samples were used. Each sample was attached to the thermoelectric cooler using mechanical screws. Calibration curve for each sample was obtained as explained in section 4.1.2. The operating voltage of the AC LED was set at 120V. The junction temperature of the package was estimated at three temperature settings (25⁰C, 50⁰C & 75⁰C) of the thermoelectric cooler as explained in section 4.1.2. Three measurements at random sequence was obtained at each temperature setting. The process was repeated for operating voltages of 110V and 130V. Optical measurements were performed at each operating condition following the protocol mentioned in appendix E.

4.3 Hypothesis 4: Variation of thermal resistance with input voltage

The hypothesis attempt to verify that between the input voltage ranges, from 110V to 130V thermal resistance will reduce with high input voltage.

4.3.1 Experiment variables

4.3.1.1 Independent variable

➤ Input voltage

AC LEDs are driven at constant voltage; therefore input electric power to the AC LED is changed by changing the rms AC voltage applied to the LED. Three input voltages of 110V, 120V and 130V were used. AC LEDs are rated to operate at 120V, but distribution grids typically allow a tolerance of $\pm 10\%$ [55]. AC LEDs if directly connected to the wall plug without an AC voltage regulator would have to operate within this tolerance.

4.3.1.2 Dependent variable

➤ The sense voltage

This is the voltage across the junction when the reference current pulse is applied at the dead-zone of the current waveform in the voltage drop method for AC LED. This is the temperature sensitive parameter that is used to predict T_j .

4.3.1.3 Extraneous variables

➤ Ambient temperature

Thermal resistance increases with ambient temperature [47]. Therefore, it is important to maintain the ambient temperature at a constant value to observe the effect of the input power. Ambient temperature is held constant by maintaining the cold plate temperature of the active thermoelectric cooler constant.

5. Results

5.1 Verification of Hypothesis 1

Thermal resistance of a GaN based white AC LED package was measured using the voltage drop method for AC LED and rms current recovery method. Calibration curve for the white AC LED sample (Figure 19) was obtained at a reference current of 0.06mA.

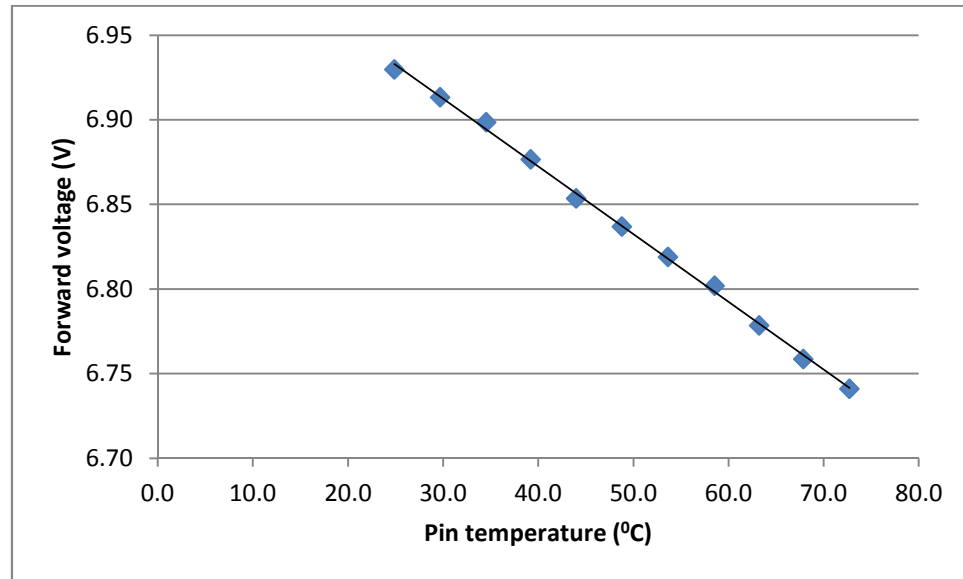


Figure 19: Calibration curve for white AC LED sample

The equation of the line of best fit is $Y = -0.0040x + 7.0325$. The temperature sensitivity of the forward voltage of the LED is $4\text{mV}/^\circ\text{C}$. It is possible to state statistically with 95% confidence that the gradient and the intercept of the calibration curve would be within the following band.

Gradient: $0.0040 \pm 0.0001 \text{ V}/^\circ\text{C}$

Intercept: $7.0325 \pm 0.0057 \text{ V}$

$R^2 = 0.99$ ($p < 0.05$), which is a strong correlation of eleven independent measurements.

* Portions of this chapter previously appeared as: A. Jayawardena, Y.-W. Liu, and N. Narendran, "Methods for estimating junction temperature of AC LEDs," in *Proc. SPIE*, vol. 8123, San Diego, CA, 2011, pp. 81230I-1-81230I-6, doi:10.1117/12.904056.

During 120V_{rms} AC operation the reference current pulse was applied at the current dead-zone and forward voltage drop across the LED was measured. Three repeated measurements were performed at three different temperature settings. The measured forward voltage was converted to T_j using the calibration curve. The estimated junction temperature values along with its standard deviation are given below in Table 1.

	25°C	50°C	75°C
Junction Temperature (°C)	42.9	70.3	100.1
Standard deviation	0.14	0.51	1.27

Table 1: Estimated junction temperature of white AC LED package at 120V

Thermal resistance was calculated using following formula,

$$R_{J-P} = \frac{(\text{Junction Temperature} - \text{Pin Temperature})}{(\text{Input Electric power} - \text{optical power})}$$

Thermal resistance calculation at each temperature setting of thermoelectric cooler using voltage drop method for AC LED is given in Table 2.

Cold plate temperature	35°C	55°C	60°C
Junction Temperature (°C)	53.3	75.1	81.1
Pin Temperature (°C)	35.8	55.1	59.8
Temperature difference(°C)	17.5	20.0	21.3
Electric Input Power (W)	2.79	2.98	3.02
Optical power (W)	0.209	0.205	0.204
Thermal Input power (W)	2.58	2.77	2.82
Thermal Resistance (°C/W)	6.8	7.2	7.6

Table 2: Thermal Resistance calculations using voltage drop method for AC LED

The rms current recovery method was used to calculate thermal resistance of the same GaN AC LED package. Three independent first half cycle rms current measurements were obtained at each temperature settings. The summary of those measurements are given in Table 3.

Temperature Setting	50°C	60°C	70°C
Average (mA)	24.142	24.716	25.664
Standard Deviation (mA)	0.098	0.121	0.144

Table 3: First half cycle rms current measurements

Based on the repeated measurement analysis the maximum standard deviation of predicted junction temperature is 2.3°C . The thermal resistance of the AC LED package was calculated by recovering the first half cycle rms current. The results are shown in Table 4. The recovered pin temperature refers to the temperature at which the first half cycle rms current of the AC LED is recovered.

Initial Cold Plate Temperature	50 $^{\circ}\text{C}$	70 $^{\circ}\text{C}$	75 $^{\circ}\text{C}$
Initial pin Temperature ($^{\circ}\text{C}$)	46.6	65.8	72
Recovered pin temperature ($^{\circ}\text{C}$)	37.4	56.9	59.8
Temperature difference ($^{\circ}\text{C}$)	9.2	8.9	12.2
Input electric (W)	2.60	2.68	2.81
Optical power (W)	0.209	0.205	0.204
Thermal input power (W)	2.4	2.5	2.6
Thermal Resistance ($^{\circ}\text{C}/\text{W}$)	3.8	3.6	4.7

Table 4: Thermal resistance calculation using rms current recovery method

The comparison of thermal resistance values calculated for the same AC LED package in Table 2 and Table 4 reveal that there is almost a 50% difference in the values, which is more than the measurement uncertainties of the two experiment set ups. The difference in pin temperature in Table 2 and recovered pin temperature in Table 4 is insignificant (less than 2°C) to create such a wide discrepancy due to the effect of ambient temperature. The difference in input thermal power to the junction is also insignificant for the two cases. Therefore, the only plausible reason for such a discrepancy would be the measurement method used.

It was hypothesized, in hypothesis 1 that the main contributing factor for this discrepancy is the temperature rise that occurs in the first half cycle of the AC current which is not accounted for in the rms current recovery method. Therefore, if this temperature rise in the junction is measured using the voltage drop method for AC LED and accounted for in the rms current recovery method, both should yield similar results. If there is any discrepancy in the calculated thermal resistance values using two methods that could be attributed to measurement uncertainties in the setups.

Temperature rise in the first half cycle of the AC current waveform at different temperature settings of the thermoelectric cooler was measured. Three repeated measurements were performed at each temperature. The results are given below in Table 5.

Cold plate temperature (°C)	25	50	60	70	75
Junction Temperature after the first half cycle (°C)	29.6	54.2	64.6	75.0	80.3
Standard Deviation (°C)	0.24	0.33	0.20	0.18	0.12

Table 5: Junction Temperature after the first half cycle of AC current

In rms current recovery method T_j should be at the values mentioned above when the current is recovered, rather than at the initial pin temperature just before turning on the AC LED. Therefore, thermal resistance should be calculated as,

$$R_{J-P} = \frac{(T_j \text{ after the first half cycle of current} - \text{recovered Pin Temperature})}{(\text{Input Electric power} - \text{optical power})}$$

Initial Cold Plate Temperature	50°C	70°C	75°C
T_j after first half cycle (°C)	54.2	74.8	80.3
Recovered pin temperature (°C)	37.4	56.9	59.8
Temperature difference (°C)	16.8	17.9	20.5
Input electric power (W)	2.60	2.68	2.81
Optical power (W)	0.209	0.205	0.204
Thermal input power (W)	2.4	2.5	2.6
Thermal Resistance (°C/W)	7.0	7.2	7.9

Table 6: Thermal resistance calculated after accounting for first half cycle heating

The comparison of thermal resistance calculated using both methods after accounting for initial half cycle junction is heating is given below in Table 7.

$R_{\theta J-P}$ Voltage drop method (°C/W)	6.8	7.2	7.6
$R_{\theta J-P}$ rms current recovery method (°C/W)	7.0	7.2	7.9
Difference (°C/W)	-0.2	0.0	-0.3
Difference %	-3	0	-4

Table 7: Comparison of thermal resistance values calculated using two methods

The difference in thermal resistance values calculated using the two measurement methods can now be explained by the measurement uncertainties in the two measurement setups. A summary of the comparison before adjusting for first half cycle heating and after adjusting for first half cycle heating is given in Figure 20 & Figure 21 respectively.

Therefore Hypothesis “*Thermal resistance values of an AC LED measured using voltage drop method for AC LED and rms current recovery method after adjusting for first half cycle heating in the junction will agree within 10%*” is verified.

A similar analysis was performed for a GaP based AC LED package at two different temperature conditions (50°C & 75°C). The summary of results is given in Table 8. The results further verify the hypothesis 1.

R_{θ_j-p} Voltage drop method (°C/W)	6.3	6.9
R_{θ_j-p} rms current recovery method (°C/W)	6.3	6.5
Difference (°C/W)	0	0.4
Difference %	0	5.7

Table 8: Comparison of thermal resistance measurements for GaP LED

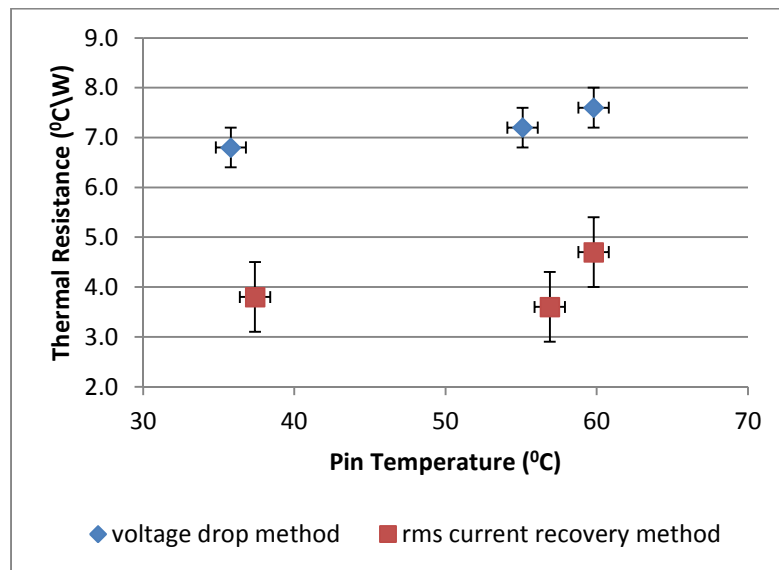


Figure 20: The comparison of thermal resistance measured using voltage drop method for AC LED and rms current recovery method before adjusting for first half cycle heating

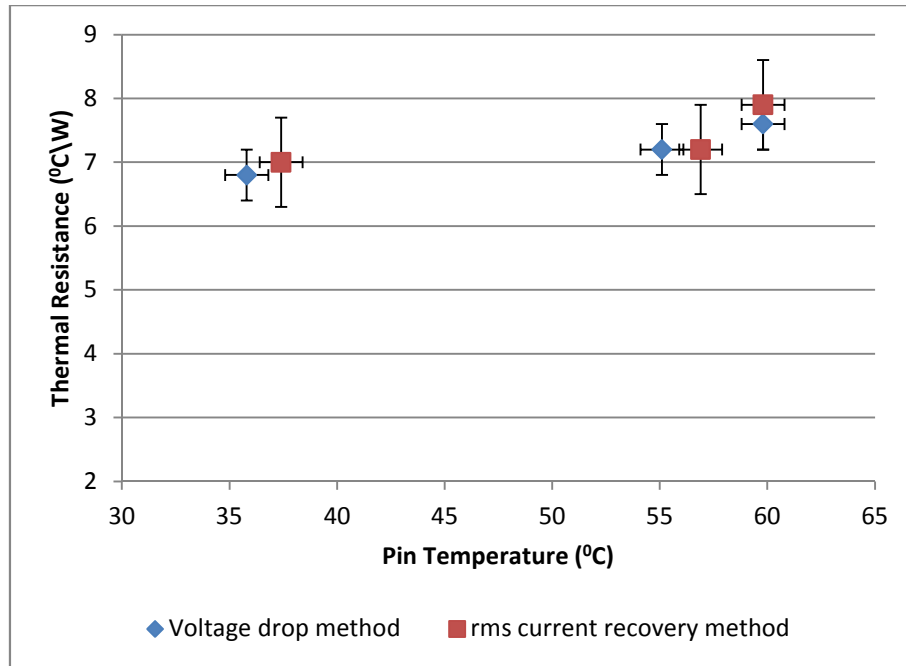


Figure 21: The comparison of thermal resistance measured using voltage drop method for AC LED and rms current recovery method after adjusting for first half cycle heating

5.2 Verification of Hypothesis 2

Thermal resistance of a GaP based LED package was measured using the voltage drop method for AC LED, following the same protocol as mentioned in chapter 4.1.3. The calibration curve that indicates the relationship between forward voltage and junction temperature for the package is given in Figure 22.

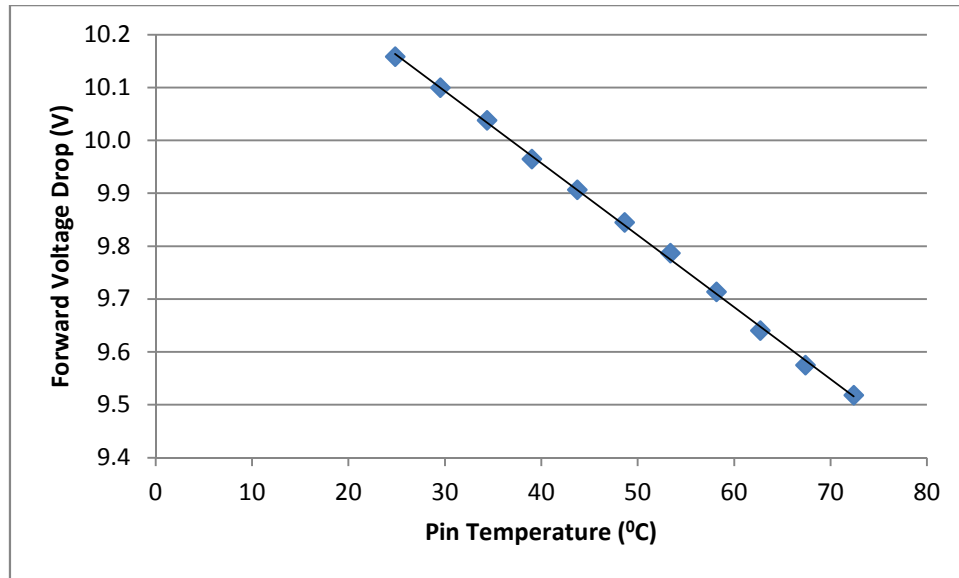


Figure 22: Calibration curve for GaP based AC LED package

The gradient and intercept of the line of best fit for the above data points along with their 95% confidence bands are given below.

$$\text{Gradient} = 0.0136 \pm 0.0003 \text{ V/}^{\circ}\text{C}$$

$$\text{Intercept} = 10.5019 \pm 0.0152 \text{ V}$$

The coefficient of correlation for the above calibration curve is 0.999, which is a statistically significant correlation for eleven independent measurements ($P < 0.05$). The package shows strong linear correlation between forward voltage and T_j , therefore satisfy the basic requirement that is necessary to use voltage drop method.

Junction temperature was measured at three different AC input voltages (110, 120V & 130V) using voltage drop method for AC LED. At each input voltage T_j was measured at three temperature settings of the thermoelectric cooler (25°C , 50°C & 75°C). The estimated T_j of the package at each input voltage and temperature combinations are given below in Table 9.

	25°C	50°C	75°C
110V	33.3°C	58.0°C	84.0°C
120V	41.8°C	67.6°C	94.0°C
130V	46.0°C	71.6°C	97.7°C

Table 9: Estimated junction temperature of GaP based AC LED package

At each of these AC input voltage and temperature combinations the peak wavelength value of the GaP based AC LED package was measured as explained in chapter 4.2.2. The measured peak wavelengths of the GaP based AC LED package are given in Table 10.

	25°C	50°C	75°C
110V	620.35nm	623.91nm	627.62nm
120V	621.49nm	625.08nm	628.91nm
130V	623.35nm	626.65nm	630.73nm

Table 10: Peak wavelength of GaP based AC LED package

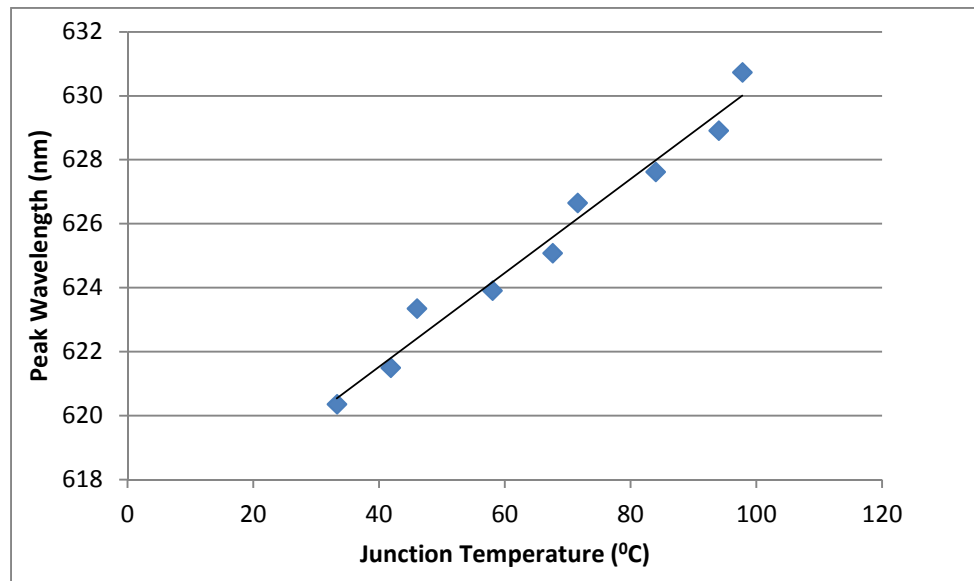


Figure 23: Relationship between junction temperature and peak wavelength for GaP based AC LED package

The gradient and intercept of the line of best fit for the data points in Figure 23 along with their 95% confidence bands are given below.

$$\text{Gradient} = 0.146 \pm 0.020 \text{ nm}^{\circ}\text{C}$$

$$\text{Intercept} = 615.65 \pm 1.40 \text{ nm}$$

The correlation coefficient (R^2) of the line of best fit is 0.9732.

The peak wavelength of the GaP based AC LED package has a statistically significant ($P < 0.05$) linear correlation with junction temperature. Therefore the hypothesis “*For GaP based ACLED package; If the junction temperature (Junction temperature is*

estimated using voltage drop method) increases then the peak wavelength will shift to longer wavelength, and the rate of peak wavelength shift with temperature will be linear” is verified.

5.3 Verification of Hypotheses 3&4

The average of three independent T_j measurements obtained at each voltage and temperature combination for sample 1 is given in Table 11.

Input Voltage	25 ^o C	50 ^o C	75 ^o C
110V	37.8 ^o C	63.9 ^o C	92.2 ^o C
120V	42.9 ^o C	70.3 ^o C	100.1 ^o C
130V	50.0 ^o C	79.0 ^o C	110.8 ^o C

Table 11: Average of estimated junction temperature for Sample 1

The thermal resistance was calculated using following formula,

$$R_{J-P} = \frac{(\text{Junction Temperature} - \text{Pin Temperature})}{(\text{Input Electric power} - \text{optical power})}$$

All the data that was collected to calculate thermal resistance of sample 1 is given in Appendix F. The thermal resistance calculated using the average T_j is shown in Table 12. All thermal resistance values have the units of ^oC/W.

	25 ^o C	50 ^o C	75 ^o C
110V	7.0	7.5	8.9
120V	6.4	7.1	8.3
130V	6.2	6.9	8.2

Table 12: Thermal resistance of sample 1

Figure 24 shows the variation of thermal resistance of sample 1 with ambient temperature at three different input AC voltages. An F-test and a pair wised comparison using t-test was performed. The results of the statistical analysis are provided in Appendix F. The results of the F-test confirmed that ambient temperature has a significant effect ($P < 0.05$) on thermal resistance. For a probability criterion of $P < 0.025$ (one tail t-test) all the compared means show a significant difference. This would mean that when the input AC voltage is held constant measured thermal resistance is

significantly different at different cold plate temperatures. As shown in Figure 24 when the cold plate temperature increases measured thermal resistance increases. Therefore for sample 1 hypothesis 3, “*In the range of 25⁰C to 75⁰C, if the ambient temperature surrounding the AC LED increases then the thermal resistance value will increase*” is verified.

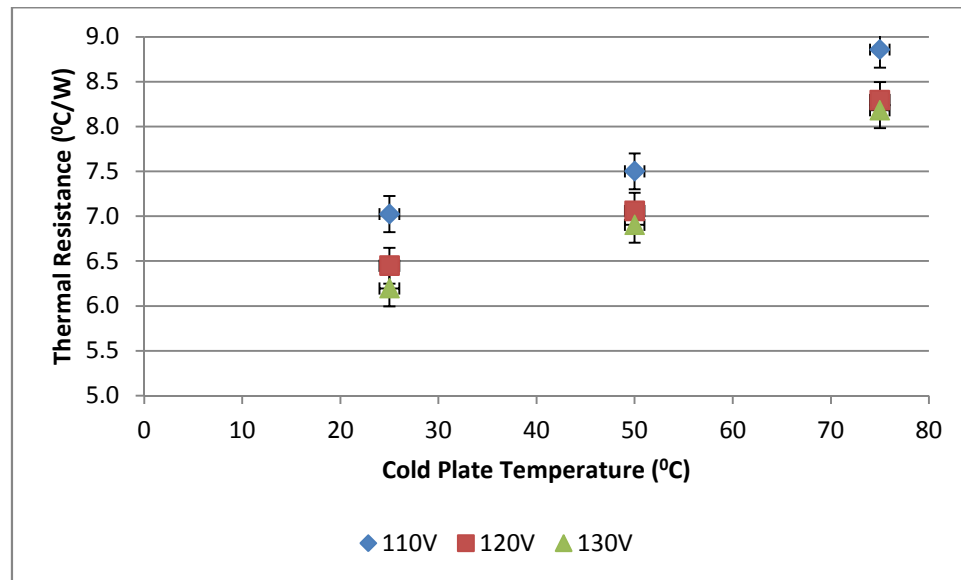


Figure 24: Variation of thermal resistance with cold plate temperature of sample 1, GaN based white AC LED package

The variation of thermal resistance with input AC voltage is shown in Figure 25. The results of the statistical analysis are given in Appendix F. The F-test showed that input AC voltage has a significant effect ($P < 0.05$) on thermal resistance. For a criterion probability of $P < 0.025$ (one tail test) part of the compared means don't show a significant difference. It is evident from the data that there is a clear thermal threshold beyond which the effect of temperature increase around the LED package nullifies the impact of reduction in thermal resistance due to high input voltage. The fact that the F-test indicated a possible interaction between temperature and AC input voltage on the thermal resistance measurement supports this argument.

Therefore even though input power has a significant effect on the thermal resistance measurement and trend of the data points in Figure 25 suggests that thermal resistance

decrease with input AC voltage. Hypothesis 4 doesn't fully explain the behaviour of thermal resistance with input power. Therefore hypothesis 4 for sample 1, "In the range of 110V-130V, if the input voltage to the AC LED increases then the thermal resistance value will decrease" is partially verified.

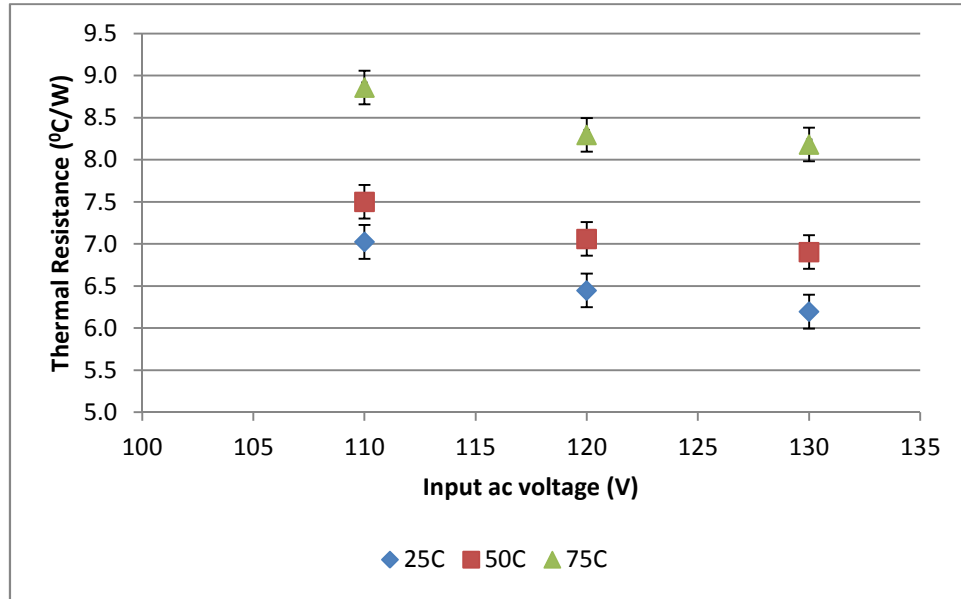


Figure 25: variation of thermal resistance with input AC voltage for sample1, GaN based white AC LED package

Similar results were observed for the sample 2. The detailed results of the 2nd GaN based white AC LED sample are given in Appendix F.

6. Discussion

Of the two methods, voltage drop method and rms current recovery method, studied in this thesis for estimating junction temperature of AC LED, the voltage drop method for AC LED emerged as the more promising candidate for junction temperature prediction. Even though the rms current recovery method gave erroneous results initially for the measured thermal resistance values, after the temperature rise in the first half cycle of the current waveform was added the thermal resistance measured using rms current recovery method and voltage drop method for AC LED yielded similar results.

6.1 Absolute junction temperature measurement

In order to further verify the accuracy of the absolute junction temperature measurement of the AC LED package, peak wavelength shift method was used. The experiment setup and protocol is explained in section 4.2.2. A calibration current of 0.06mA was chosen since at this current there is negligible heating in the junction. The methodology adopted in choosing this reference current is explained in detail in section 4.2.2. The calibration curve for the GaP based AC LED package is shown in Figure 26.

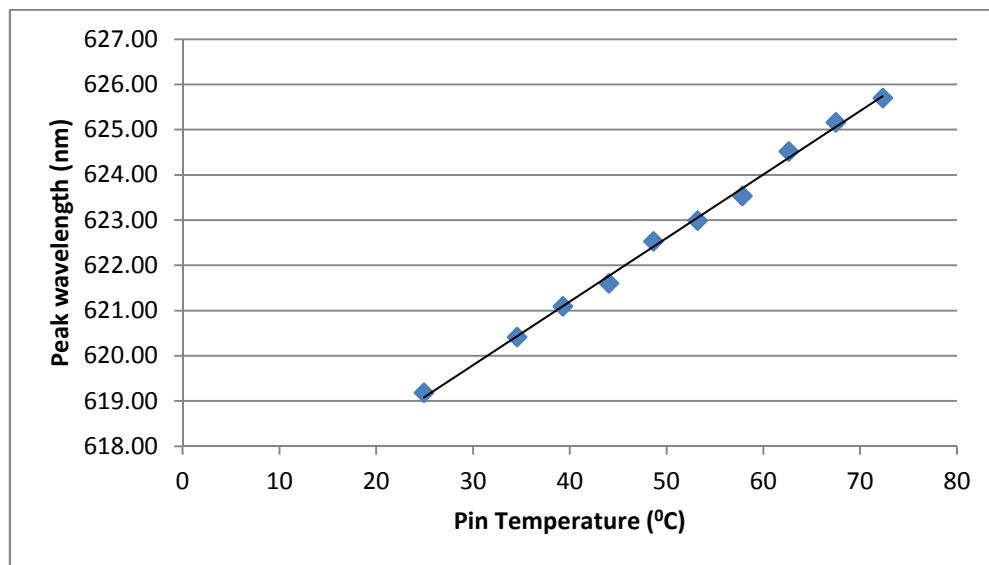


Figure 26: Calibration curve for peak wavelength shift method

The line of best fit for the calibration curve along with their tolerances in the 95% confidence interval band is as given below.

Gradient: $0.1405 \pm 0.0059 \text{ nm}^\circ\text{C}$

Intercept: $615.58 \pm 0.31 \text{ nm}$

Figure 27 shows the peak wavelength plotted against the junction temperature estimated using voltage drop method and peak wavelength shift method. The dotted straight line connects the data points that represent the estimated T_j (using peak wavelength shift method) at each peak wavelength. The line of best fit drawn, connecting the data points that represents T_j estimated using voltage drop method at each peak wavelength is also presented in the Figure 27.

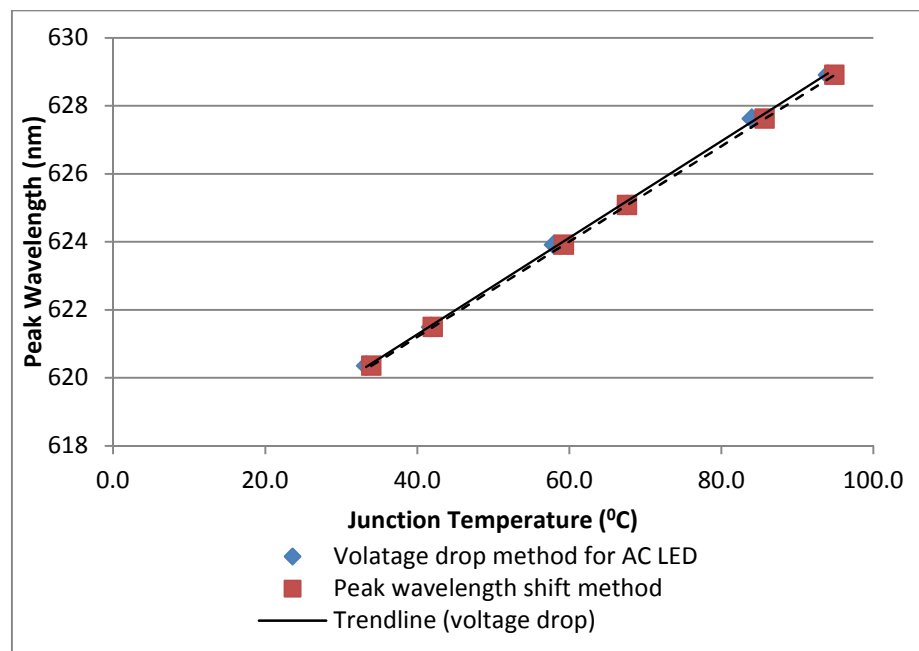


Figure 27: Peak wavelengths vs. estimated T_j using voltage drop method for AC LED and peak wavelength shift method

The equation of the trend line (voltage drop) in Figure 27 that was drawn through the points that represents the T_j estimated using voltage drop method for AC LED is,

$$y = 0.1421x + 615.59$$

The R^2 value of the line of best fit is 0.9994

The above trend line (voltage drop) equation was compared to the equation of the trend line (peak wavelength) in Figure 27, which is same as the equation of the peak wavelength calibration curve in Figure 26. The slope and intercept of the trend line (voltage drop) is within the 95% confidence band of the slope and intercept of the peak wavelength calibration curve in Figure 26. Therefore statistically it could be stated that both trend lines overlap on one another and their offset as observed in Figure 27 is due to the measurement uncertainties of the experiment set ups.

The Table 13 shows a comparison of estimated T_j using two methods. The calculated difference between the two methods are well within the measurement tolerances of the two set ups. The measurement uncertainty of T_j estimated using peak wavelength shift method is $\pm 1.4^{\circ}\text{C}$. The measurement uncertainty of T_j estimated using the voltage drop method is $\pm 1.35^{\circ}\text{C}$. However there is a systematic difference that suggests that voltage drop method underestimate the junction temperature. This is consistent with what Yang, et.al [39], observed in their comparative study of voltage drop method and peak wavelength shift method for DC LEDs. This may be due to following reasons,

- The capacitance in the junction causes voltage measured to lag behind the junction temperature.

This is a phenomenon that is well described in literature for junction temperature measurement of semiconductor packages [43]. Therefore it is plausible that estimated junction temperature using voltage drop method is lower than its real value.

- A sampling delay time was built in to the voltage drop measurement set up to avoid initial electrical noise that occurs during the switching.

This delay would mean that the sampled voltage represents a junction that is cooled for a 1ms duration. The assumption that was made in the voltage drop method is that when the AC LED reached its thermal stability the junction doesn't cool down in the current dead-zone due to thermal capacitance of the package. Thermal stability criterion was determined by measuring the pin temperature rather than the junction temperature. It is possible that even though the pin of the LED package has achieved thermal stability junction has not reached its thermal stability and still undergoes some amount of cooling

in the current dead-zone. Therefore due to sampling delay time measured voltage represents a slightly cooled junction.

Peak Wavelength (nm)	T _j estimated using Peak wavelength shift method (°C)	T _j estimated using voltage drop method (°C)	Difference (°C)
620.35	34.0	33.3	0.7
623.91	59.3	58.0	1.3
627.62	85.7	84.0	1.7
621.49	42.1	41.8	0.2
625.08	67.6	67.6	0.0
628.91	94.9	94.0	0.9

Table 13: Comparison of junction temperature measurements using voltage drop and peak wavelength shift methods

6.2 Measurement Uncertainty: voltage drop method

A point of concern when implementing any measurement scheme is repeatability of results when measured over a period of time and in similar environment conditions. Possible source of errors in the voltage drop method is identified in this section.

6.2.1 Calibration curve

The slope and intercept of the calibration curve is bound to vary between different samples of the identical product family. For example two AC LED samples of the same manufacturer that were tested in the voltage drop set up had temperature sensitive parameters of 4mV/°C and 4.3mV/°C. Therefore if only a single sample of a batch is calibrated and the same calibration curve is used for the entire batch this variation in gradient would produce 7% uncertainty in the measured temperature rise in a junction.

The gradient of the voltage calibration curve in the voltage drop method if properly measured is an intrinsic property of the package. Therefore more homogeneous the packages are less the variability of gradient between packages of the same product family. Further analysis with greater sample size drawn from a same batch of AC LEDs

is needed for a detailed analysis of uncertainty of T_j measurements performed using a single or few samples drawn out of a batch of LEDs.

Another source of error during calibration is the drift of reference current during calibration. If a latest source measurement unit (ex: National Instrument PXI-4130, Agilent B2902A) was used as the source to provide the reference current of $60\mu\text{A}$ the drift could vary from 0.06% [56] to 0.19% [57].

The intercept of the calibration curve is dependent on the thermal environment surrounding the LED package. Therefore the uncertainty of the intercept of the calibration curve is much larger than the uncertainty of the gradient. In the case of DC LEDs this uncertainty is minimized by placing the device under test in a temperature controlled chamber [9]. The voltage drop method for DC LEDs also measures the voltage drop that occurs when current across the LED switches from heating current to measurement current. By taking a voltage measurement just prior to the application of measurement current and taking the difference between the voltage at heating current and measurement current, the T_j measurement doesn't have to rely on a predefined intercept value that was obtained during calibration. This option is not available for AC LEDs, because the forward bias of the AC LED changes rapidly with AC input voltage.

6.2.2 Thermal environment

The traditional thermal environments used for semiconductor device calibrations are either ovens or die-electric liquid baths [43,9]. In the recent past several studies on T_j measurements use thermoelectric coolers to generate the required thermal environment for calibration [14,2,58]. Thermoelectric coolers offer a fast and reliable way to achieve a stable temperature surrounding for LEDs. However unlike in the case of ovens or die electric baths thermoelectric cooler cannot ensure that the entire thermal environment surrounding the LED is at a uniform stabilized temperature.

It was assumed during calibration that thermal environment that is immediately surrounding the LED is influenced solely by the thermoelectric cooler and ambient air temperature and velocity has negligible effect on the AC LED. The results of this thesis and measurement standards on DC LEDs highlight the importance of maintaining a similar thermal environment during thermal resistance measurements [9,29]. Thermoelectric cooling is hardly employed as a thermal management strategy for LEDs. An advantage of the voltage drop method for AC LED compared to rms current recovery methods is that it doesn't mandate you to use a thermoelectric cooling system. It enables the measurement of thermal resistance in similar thermal environments as the AC LED will be used.

6.2.3 Pin temperature measurement

Thermal resistance value is often specified with respect to a reference point on the board of the LED package. This is one of the major sources of errors in the thermal resistance measurement. Different thermocouple types have significant measurement uncertainties in the temperature range of interest for LED packages. Table 14 list the maximum error of thermocouples that meet the IEC 584-2 (1982) standard at 0-200⁰C temperature range.

Thermocouple Type	error (⁰ C)
J type	1.5
T Type	0.8
S type	1.0
K Type	1.5

Table 14: Standard errors of thermocouple types

Selection of a reference point to measure the pin temperature is another source of error. It is assumed that the board of the LED package is an isothermal surface but this is far from reality. Depending on the point at which the thermocouple is attached on the board the measured pin temperature would be different, and therefore it would be difficult to reproduce the measurement results universally, unless the thermocouple is attached at the exact same location.

In order to remove this error from the thermal resistance measurement, literature has suggested the use of the cold plate temperature of the thermoelectric cooler as the reference. Cold plate if properly designed would be closest to an isothermal surface, and the temperature of that could be measured using a thermistor which typically has measurement errors of only 0.15°C to 0.3°C depending on the type of the metal and class. The use of cold plate temperature would make the thermal resistance measurements reproducible when measured in different laboratories.

Another strategy suggested in literature to measure thermal resistance by avoiding the pin temperature measurement is to use temporal difference in junction temperature instead of using spatial difference of temperature [41].

6.2.4 The uncertainty analysis

An uncertainty analysis was performed for each measurement set up using the propagation of error formulas [59]. The uncertainty analysis is explained in detail in Appendix G. The summary of the uncertainty analysis is given below in Table 15.

Measurement method	Junction Temperature (T_j)	Thermal Resistance (SD within 95% confidence)
Voltage drop method	$\pm 1.35^{\circ}\text{C}$	$\pm 0.4^{\circ}\text{C/W}$ ($\pm 5.5\%$)
Rms current recovery using active heat sink	$\pm 2.3^{\circ}\text{C}$	$\pm 0.7^{\circ}\text{C/W}$ ($\pm 10\%$)
Peak wavelength shift	$\pm 1.4^{\circ}\text{C}$	$\pm 0.5^{\circ}\text{C/W}$ ($\pm 10\%$)

Table 15: Summary of the uncertainty analysis

6.3 In line measurement of AC LED packages

The LED industry uses an optical pulse method, where a 10ms current pulse is applied to the LED package for inline measurement of light output characteristics [58]. The assumption being that T_j doesn't increase substantially during this period. Therefore, data sheets specify optical characteristics of LEDs at 25⁰C. Optical pulse measurements require a certain integration time. Therefore the assumption that there is no self-heating in the junction during optical measurements is not valid [14]. According to Poppe et.al [58], during this 10ms period, with similar thermal boundary conditions prevalent in an inline measuring environment when a 350mA current pulse is applied T_j change by 15⁰C. Therefore measurement of T_j when obtaining optical measurements is important for accurate binning.

The 10ms time frame in the case of AC LEDs represents approximately half a cycle of AC voltage (60Hz waveform 8.3ms). In order to implement voltage drop method as an in-line measurement procedure a batch calibration needs to be performed to obtain the calibration factor. As discussed in section 6.2.1, since intercept of the calibration curve is dependent on the thermal environment at the point of measurement, its use in T_j measurement should be avoided. Instead a reference current pulse can be applied at the start of the AC measurement. After running the AC LED a given number of cycles, another reference current pulse can be applied. By taking the temporal voltage difference between the initial and final reference current pulses, the temperature rise in the junction could be estimated.

7. Conclusion

This thesis further developed the voltage drop method for AC LED packages introduced in literature [3]. This thesis demonstrated, the thermal resistance measured using rms current recovery method [2] is similar to the the thermal resistance measured using the voltage drop method for AC LED if the junction heating that occurs during the first half cycle of current is accounted for.

The validity of the voltage drop method for AC LED in predicting T_j of an AC LED was further proved by measuring the peak wavelength value of a GaP based AC LED emission spectrum. The peak wavelengths of the package showed a strong correlation with T_j estimated using the voltage drop method for AC LED. The absolute T_j measured using voltage drop method for AC LED and peak wavelength shift method agree very well.

It should be noted that the estimated T_j is the average temperature of all junctions in an AC LED package during its AC operation. The thesis also measured the heating profile of the junction in the first half cycle of AC current. This thesis explains in detail the voltage drop method for AC LED emphasizing the potential sources of errors, and possible ways to avoid them.

The thermal resistance of AC LED packages at different ambient temperature and input voltage conditions were measured. All thermal resistance values were calculated by using the effective power dissipated at the junction (total power minus the optical power) of the package at different input voltage and temperature conditions. The data showed influence of both temperature and input voltage on the thermal resistance. When the ambient temperature was raised the thermal resistance value increased. This is consistent with the similar studies in literature for DC LEDs [47,49]. The heat spreading that occurs in the board of the LED package makes it difficult to separate thermal resistance due to conduction and convection [45] . Therefore the measured junction to pin conduction thermal resistance is not completely independent from the pin to ambient convective thermal resistance. Another plausible reason could be that 1-D conduction

heat transfer assumption made during estimating thermal resistance is an over simplification of a 3-D heat transfer that occurs in a package.

The thesis results showed that the thermal resistance of an AC LED package is also influenced by the input power to the package. However the results showed that at high ambient temperature conditions there is no significant difference between the thermal resistances measured at different input power levels. When the input power to the package is increased there are two opposing influences on the thermal resistance of the package. High input power leads to high temperature in the junction, and hence the area surrounding the package, thereby increasing the thermal resistance as explained above. On the other hand high input voltage leads to more heat dissipation in the external series resistance of the package there by reducing the estimated thermal resistance [46]. The data suggests that at high ambient temperatures thermal effect negates the input voltage effect on thermal resistance.

8. Bibliography

- [1] F.-S. Hwu, G.-J. Sheu, M.-T. Lin, and J.-C. Chen, "Method for determining the junction temperature of alternating current light-emitting diodes," *IET Sci. Meas. Technol.*, vol. 3, no. 2, pp. 159-164, Mar. 2009, doi: 10.1049/iet-smt:20080096.
- [2] Y. Zong, P.-T. Chou, M.-T. Lin, and Y. Ohno, "Practical method for measurement of AC-driven LEDs at a given junction temperature by using active heat sinks," in *Proc. SPIE*, vol. 7422, San Diego, CA, 2009, pp. 742208-1 - 742208-7, doi:10.1117/12.826743.
- [3] Y.-W. Liu, A. Jayawardena, T. R. Klein, and N. Narendran, "Estimating the junction temperature of AC LEDs," in *Proc. SPIE*, vol. 7784, San Diego, CA, 2010, pp. 778409-1- 778409-6, doi: 10.1117/12.863060.
- [4] A. Poppe, G. Farkas, T. Temesvölgyi, B. Katona, and G. Molnár, "Thermal impedance of AC LEDs," in *16th Int. Workshop on Thermal Investigations of ICs and Systems 2010*, Barcelona, 2010, pp. 1-6.
- [5] Navigant Consulting Inc., "Energy saving estimates of light emitting diodes in niche lighting applications," Building Technologies Program, Office of Energy Efficiency and Renewable Energy, U.S. Department of Energy, Washington, D.C., 2008.
- [6] H.-H. Yen, W.-Y. Yeh, and H.-C. Kuo, "GaN alternating current light-emitting device," *Phys. Stat. Sol. (a)*, vol. 204, no. 6, pp. 2077-2081, Jun. 2007, doi: 10.1002/pssa.200674766.
- [7] N. Narendran, Y. Gu, J. P. Freyssonier, H. Yu, and L. Deng, "Solid-state lighting: failure analysis of white LEDs," *J. Crystal Growth*, vol. 268, no. 3-4, pp. 449-456, Aug. 2004, doi:10.1016/j.jcrysgr.2004.04.071.
- [8] D. L. Barton, M. Osinski, P. Perlin, C. J. Helms, and N. H. Berg, "Life tests and failure mechanisms of GaN/AlGaIn/InGaIn light-emitting diodes," in *Proc. SPIE*, vol. 3279, San Jose, CA, 1998, doi:10.1117/12.304426.
- [9] *Integrated Circuits Thermal Measurement Method-Electrical Test Method (Single Semiconductor Device)*, JESD51-1, Dec. 1995.

- [10] G. Farkas, Qv. V. Vader, A. Poppe, and G. Bognár, "Thermal investigation of high power optical devices by transient testing," *IEEE Trans. Compon. Packag. Technol.*, vol. 28, no. 1, pp. 45-50, Mar. 2005, doi:10.1109/TCAPT.2004.843197.
- [11] E. Hong and N. Narendran, "A method for projecting useful life of LED lighting systems," in *Proc. SPIE*, vol. 5187, San Diego, CA, 2004, pp. 93-99, doi:10.1117/12.509682.
- [12] N. Narendran and Y. Gu, "A non-contact method for determining junction temperature of phosphor converted white LEDs," in *Proc. SPIE*, vol. 5187, San Diego, CA, 2004, pp. 107-114, doi:10.1117/12.509751.
- [13] W. J. Hwang, T. H. Lee, L. Kim, and M. W. Shin, "Determination of junction temperature and thermal resistance in the GaN-based LEDs using direct temperature measurement," *Phys. Stat. Sol. (c)*, vol. 1, no. 10, pp. 2429-2432, Sep. 2004, doi: 10.1002/pssc.200405098.
- [14] Y. Zong and Y. Ohno, "New practical method for measurement of high-power LEDs," in *Proc. CIE Expert Symp. 2008 Advances in Photometry and Colorimetry*, Turin, 2008, pp. 102-106.
- [15] N. Narendran, "Improved performance white LED," in *Proc. SPIE*, vol. 5941, San Diego, CA, 2005, pp. 594108-1-594108-6, doi:10.1117/12.625921.
- [16] Y. Narukawa, J. Narita, T. Sakamoto, and K. Deguchi, "Ultra-high efficiency white light emitting diodes," *Jpn. J. Appl. Phys.*, vol. 45, no. 41, pp. L1084 – L1086, Oct. 2006, doi: 10.1143/JJAP.45.L1084.
- [17] E. F. Schubert, T. Gessmann, and J. K. Kim, "Light emitting diodes," in *Kirk-Othmer Encyclopedia of Chemical Technology*, Jul. 2005, doi:10.1002/0471238961.1209070811091908.a01.pub2.
- [18] *The Photonic Dictionary*, 46th ed., Laurin Publishing, Pittsfield, MA, 2000, pp. D-12.
- [19] S. Nakamura, M. Takashi, and M. Senoh, "High power GaN P-N junction blue-light-emitting diodes," *Jpn. J. Appl. Phys.*, vol. 30, no. 12A, pp. L1998-L2001, Dec. 1991, doi:10.1143/JJAP.30.L1998.

- [20] A. A. Bergh and P. J. Dean, "Light-emitting diodes," in *Proc. IEEE*, vol. 60, 1972, pp. 156-223, doi: 10.1109/PROC.1972.8592.
- [21] S. M. Spitzer, N. E. Schumaker, L. A. Koszi, and J. C. North, "Multijunction AC or DC integrated GaP light emitting diode array," *IEEE Trans. Electron Devices*, vol. 22, no. 09, pp. 701-706, Sep. 1975, doi:10.1109/T-ED.1975.18206.
- [22] J.-P. Ao et al., "Monolithic blue LED series arrays for high-voltage AC operation," *Phys. Stat. Sol. (a)*, vol. 194, no. 2, pp. 376-379, Dec. 2002, doi: 10.1002/1521-396X(200212)194:23.0.CO;2-3.
- [23] T. Tamura, T. Setomoto, and T. Taguchi, "Illumination characteristics of lighting array using 10 candela-class white LEDs under AC 100 V operation," *J. Luminescence*, vol. 87-89, pp. 1180-1182, May 2000, doi:10.1016/S0022-2313(99)00588-8.
- [24] T. Sugahara et al., "Direct evidence that dislocations are non-radiative recombination centers in GaN," *Jpn. J. Appl. Phys.*, vol. 37, no. 4A, pp. L398-L400, Feb. 1998, doi: 10.1143/JJAP.37.L398.
- [25] Y. C. Shen et al., "Auger recombination in InGaN measured by photoluminescence," *Appl. Phys. Lett.*, vol. 91, no. 14, pp. 141101-3, Oct. 2007, doi:10.1063/1.2785135.
- [26] J. Hu, L. Yang, and M. W. Shin, "Mechanism and thermal effect of delamination in light-emitting diode packages," *Microelectronics J.*, vol. 38, no. 2, pp. 157-163, Feb. 2007, doi:10.1016/j.mejo.2006.08.001.
- [27] Y.-C. Hsu et al., "Failure mechanisms associated with lens shape of high-power LED modules in aging test," *IEEE Trans. Electron Devices*, vol. 55, no. 02, pp. 689-694, Feb. 2008, doi: 10.1109/TED.2007.911905.
- [28] B. Siegel, "Practical considerations in high power LED junction temperature measurements," in *Proc. 31st Int. Conf. Electronics Manufacturing and Technology*, Petaling Jaya, 2006, pp. 62-66, doi:10.1109/IEMT.2006.4456416.
- [29] *Test Methods for Semiconductor Devices*, MIL-STD-750E, 2006.

- [30] A. S. Grove, *Physics and Technology of Semiconductor Devices*. New York: John Wiley & Sons Inc., 1967.
- [31] P. E. Gray and C. L. Searle, *Electronic Principles: Physics, Models & Circuits*. New York: John Wiley & Sons Inc., 1969.
- [32] Y. P. Varshni, "Temperature dependence of the energy gap in semiconductors," *Physica*, vol. 34, no. 1, pp. 149-154, 1967, doi:10.1016/0031-8914(67)90062-6.
- [33] S. Nakamura, "The roles of structural imperfections in InGaN-based blue light-emitting diodes and laser diodes," *Science*, vol. 281, no. 5379, pp. 956-961, Aug. 1998, doi: 10.1126/science.281.5379.956.
- [34] S. Chhajed et al., "Junction temperature in light-emitting diodes assessed by different methods," in *Proc. SPIE*, vol. 5739, San Jose, CA, 2005, pp. 16-24, doi:10.1117/12.593696.
- [35] T. Takeuchi et al., "Determination of piezoelectric fields in strained GaInN quantum wells using the quantum-confined Stark effect," *Appl. Phys. Lett.*, vol. 73, no. 12, pp. 1691-1693, Jul. 1998, doi:10.1063/1.122247.
- [36] D. A. B. Miller et al., "Band-edge electroabsorption in quantum well structures: the quantum-confined stark effect," *Phys. Rev. Lett.*, vol. 53, no. 22, pp. 2173-2176, Nov. 1984, doi:10.1103/PhysRevLett.53.2173.
- [37] D. L. Smith and C. Mailhot, "Optical properties of strained-layer superlattices with Growth axis along [111]," *Phys. Rev. Lett.*, vol. 58, no. 12, pp. 1264-1267, Mar. 1987, doi:10.1103/PhysRevLett.58.1264.
- [38] E. Hong, "A non-contact method to determine junction temperature of high brightness AlGaInP light emitting diodes," M.S. thesis, Architecture, Rensselaer Polytechnic Institute, Troy, NY, 2003.
- [39] Y. K. Yang, W. C. Lien, Y. C. Huang, and N. C. Chen, "Junction temperature measurement of light-emitting diodes by voltage-temperature relation method," in *Conf. Lasers and Electro-Optics - Pacific Rim, 2007*, Seoul, 2007, pp. 1-2, doi: 10.1109/CLEOPR.2007.4391713.

- [40] A. Poppe, B. Siegal, and G. Farkas, "Issues of thermal testing of AC LEDs," in *Proc. 27th Annu. IEEE Semiconductor Thermal Measurement and Management Symp. 2011*, San Jose, CA, 2011, pp. 297-303, doi:10.1109/STHERM.2011.5767214.
- [41] A. Poppe and C. J. M. Lasance, "On the standardization of thermal characterization of LEDs," in *Proc. 25th Annu. IEEE Semiconductor Thermal Measurement and Management Symp. 2009*, San Jose, CA, 2009, pp. 151-158, doi:10.1109/STHERM.2009.4810757.
- [42] C. J. M. Lasance, "On the standardisation of thermal characterisation of LEDs part I: comparison with IC packages and proposal for action," in *14th Int. workshop Thermal Investigation of ICs and Systems, 2008*, Rome, 2008, pp. 208-212, doi:10.1109/THERMINIC.2008.4669910.
- [43] J. W. Sofia. (1995). *Fundamentals of Thermal Resistance Measurement* [Online]. Available:<http://ssl.xmu.edu.cn/download%5CThermal%5CFundamentals%20of%20Thermal%20Resistance%20Measurement.pdf>. Date Last Accessed 11/01/2011.
- [44] CREE Inc. (2011). *XLAMP XR Family Thermal Management* [Online]. Available: <http://www.cree.com/products/pdf/XLampThermalManagement.pdf>. Date Last Accessed 11/15/2011
- [45] A. Poppe and C. J. M. Lasance, "On the standardisation of thermal characterisation of LEDs part II: problem definition and potential solutions," in *14th Int. Workshop Thermal Investigation of ICs and Systems, 2008*, Rome, 2008, pp. 213-219, doi:10.1109/THERMINIC.2008.4669911.
- [46] L. Yang, J. Hu, L. Kim, and M. W. Shin, "Variation of thermal resistance with input power in LEDs," *Phys. Stat. Sol. (c)*, vol. 3, no. 6, pp. 2187-2190, May 2006, doi:10.1002/pssc.200565169.
- [47] L. Jayasinghe, Y. Gu, and N. Narendran, "Characterization of thermal resistance coefficient of high-power LEDs," in *Proc. SPIE*, vol. 6337, San Diego, CA, 2006, pp. 63370V-1-63370V-10, doi:10.1117/12.682585.

- [48] L. Jayasinghe, N. Narendran, and T. Dong, "Is the thermal resistance coefficient of high-power LEDs constant?," in *Proc. SPIE*, vol. 6669, San Diego, CA, 2007, pp. 666911-1 - 666911-6, doi:10.1117/12.738739.
- [49] S.-H. Kuo et al., "Characteristics of thermal resistance for high power LEDs," in *10th Electronics Packaging Technology Conf. 2008*, Singapore, 2008, pp. 149-154, 2008, doi: 10.1109/EPTC.2008.4763426.
- [50] M. W. Shin and L. Kim, "Thermal resistance measurement of LED package with multichip," *IEEE Trans. Compon. Packag. Technol.*, vol. 30, no. 4, pp. 632-636, Dec. 2007, doi:10.1109/TCAPT.2007.906332.
- [51] Agilent Technologies Inc. (1997, Oct.). *User Guide HP34970A Data Acquisition/Switch Unit* [Online]. Available: <http://cp.literature.agilent.com/litweb/pdf/34970-90002.pdf>. Date Last Accessed 11/05/2011.
- [52] Agilent Technologies Inc. (2011, Oct.). *Agilent 34401A Multimeter Product Overview* [Online]. Available: <http://cp.literature.agilent.com/litweb/pdf/5968-0162EN.pdf>. Date Last Accessed 11/05/2011.
- [53] Yokogawa Corp. (2002). *WT210/WT230 Digital Power Meters* [Online]. Available: http://c418683.r83.cf2.rackcdn.com/uploaded/bu7604_00e_020.pdf. Date Last Accessed 11/05/2011.
- [54] National Instruments Corp. (2010, Jun.) *Thermocouple Accuracy Table by Type and Temperature* [Online]. Available: <http://digital.ni.com/public.nsf/allkb/776AB03E065228408625727B00034E20>. Date Last Accessed 11/05/2011.
- [55] Vanguard Power (Hong Kong) Limited. (2011). *Voltage Levels Around the World* [Online]. Available: <http://www.vanguardspower.com/en/content/voltage-levels-around-world>. Date Last Accessed 11/01/2011.
- [56] Agilent Technologies Inc. (2011). *B2902A Precision Source/Measure Unit* [Online]. Available: <http://www.home.agilent.com/agilent/product.jsp?nid=-33504.978795.00&cc=US&lc=eng>. Date Last Accessed 11/05/2011.

- [57] National Instruments Corp. (2011). *NI PXI-4130* [Online]. Available: http://www.ni.com/pdf/products/us/cat_Ni_4130.pdf. Date Last Accessed 11/05/2011.
- [58] A. Poppe et al., "Emerging standard for thermal testing of power LEDs and its possible implementation," in *Proc. SPIE*, vol. 7784, San Diego, 2010, pp. 778414-1-778414-15, doi:10.1117/12.864054.
- [59] National Institute of Standards and Technology. (2010, Jun.). *NIST/SEMATECH E-Handbook of Statistical Methods* [Online]. Available: <http://www.itl.nist.gov/div898/handbook>. Date Last Accessed 07/20/2011.
- [60] C. H. Chen, W. L. Tsai, and M.Y. Tsai, "Thermal resistance and reliability of low-cost high-power LED packages under WHTOL test," in *Int. Conf. Electronic Materials and Packaging, 2008*, Taipei, 2008, pp. 271-276, doi:10.1109/EMAP.2008.4784281.
- [61] T. Zahner, "Thermal management and thermal resistance of high power LEDs," in *13th Int. Workshop Thermal Investigation ICs and Systems, 2007*, Budapest, 2007, p. 195, doi: 10.1109/THERMINIC.2007.4451776.
- [62] P.-T. Chou et al., "Development of on-chip AC LED lighting technology at ITRI," in *Proc. CIE Midterm Conf. Light and Lighting 2009*, Budapest, 2009.
- [63] A. Jayawardena, Y.-W. Liu, and N. Narendran, "Methods for estimating junction temperature of AC LEDs," in *Proc. SPIE*, vol. 8123, San Diego, CA, 2011, pp. 81230I-1-81230I-6, doi:10.1117/12.904056.

1

Appendix A: Forward voltage drop method

The standard published by JEDEC (Joint Electron Device Engineering council) in partnership with EIA (Electronic Industries Alliance) for Integrated Circuits Thermal Measurement Method – Electrical Test Method (EIA/JESD51-1) explains, the guidelines that need to be followed when measuring junction temperature using this two current forward voltage drop method.

The calibration constant (K-factor) is calculated by applying the measurement current at a controlled ambient temperature environment. The junction temperature is assumed to be equal to ambient temperature when the measurement current is applied, since it is too small to cause self-heating in the device [9].

$$K = \frac{(T_{HI} - T_{LO})}{(V_{HI} - V_{LO})}$$

where,

T_{HI} & T_{LO} – High and low ambient temperatures ($^{\circ}\text{C}$)

V_{HI} & V_{LO} – Corresponding high and low voltages at the measurement current (V)

When computing the K-factor it should be verified whether the device being tested has a linear relationship between the forward voltage and T_j . This method enables the manufacturer to perform a batch calibration. If the distribution between the samples, within a batch is acceptable; this method could be applied as an inline testing solution.

The test protocol adopted in this method could be summarized into the following three steps [9].

- Measurement current, I_M is applied and the junction voltage of the LED at this current (V_F) is recorded. A calibration curve is obtained as shown in Figure 28 (a). Figure 28: Illustration of forward voltage drop method for DC LEDs
- Heating current, I_H (designed driving current of the LED) is applied for a time duration that is sufficiently long enough to attain thermal steady state for the

device. Heating curve for the LED needs to be established prior to testing in order to establish the required heating time.

- Diode voltage (V_H) is measured at the steady state to determine the power dissipation of the diode.
- Heating current (I_H) is replaced with the measurement current (I_M), and the forward biased voltage (V_M) of the diode is measured as shown in Figure 28(b). When obtaining measurement it is important to analyze the cooling curve of the LED, to determine the required measurement delay time.

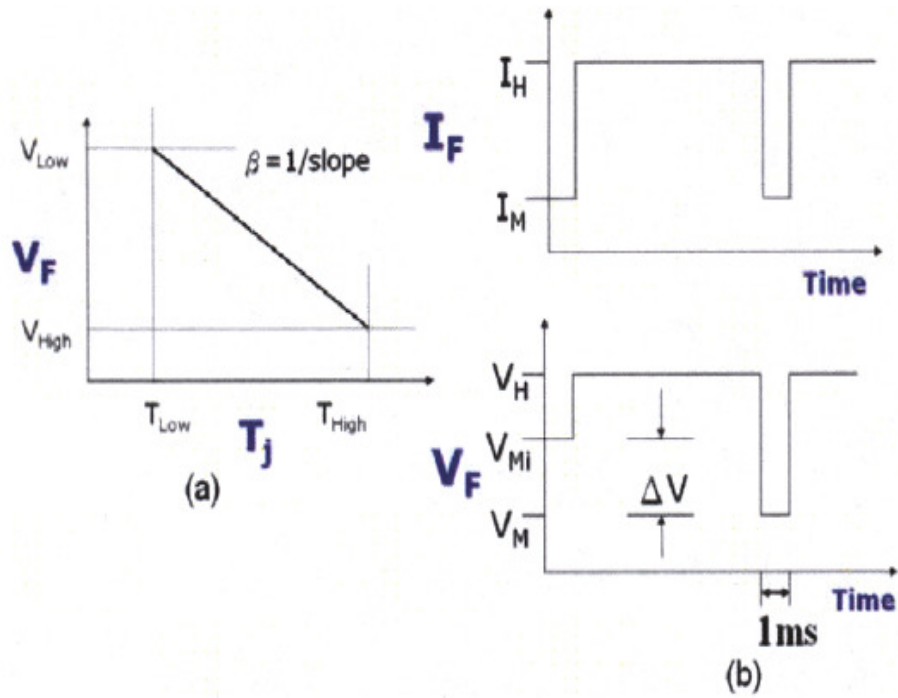


Figure 28: Illustration of forward voltage drop method for DC LEDs [60]

(a) Calibration curve of the forward voltage vs. junction temperature.

(b) Graph above: current is switched from heating current (I_H) to measurement current (I_M). Graph below: forward voltage change during transition from I_H to I_M

Appendix B: Forward voltage recovery method

The forward voltage recovery method was suggested as a possible alternative for the forward voltage drop method that is used to measure T_j of DC LEDs. According to Zong, et.al, the main advantage of this method is that unlike in the case of forward voltage drop method it doesn't require a calibration [14].

This method uses a thermoelectric cooler to control the immediate thermal environment of the DC LED. The DC LED is attached to the thermoelectric cooler using mechanical screws. When mounted on the thermoelectric cooler, it will have a T_j that is equal to the temperature of the cold plate when it's in the off state. Then the DC LED is turned on and is allowed to thermally stabilize at its rated operating current. The instantaneous forward voltage is measured at the instance of forward biasing the DC LED. The forward voltage of the LED drops rapidly as shown in Figure 29. Zong et.al, suggests to apply a stream of pulses as in Figure 30 (b) or to extrapolating the instantaneous voltage using the heating curve as in Figure 30 (c), to improve the accuracy of the initial forward voltage measurement [14].

Once the DC LED is thermally stable, temperature of the thermoelectric cooler is incrementally reduced till the forward voltage of the DC LED is equal to the measured instantaneous voltage. Once the voltage is recovered it was deduced that T_j is similar to the initial temperature [14].

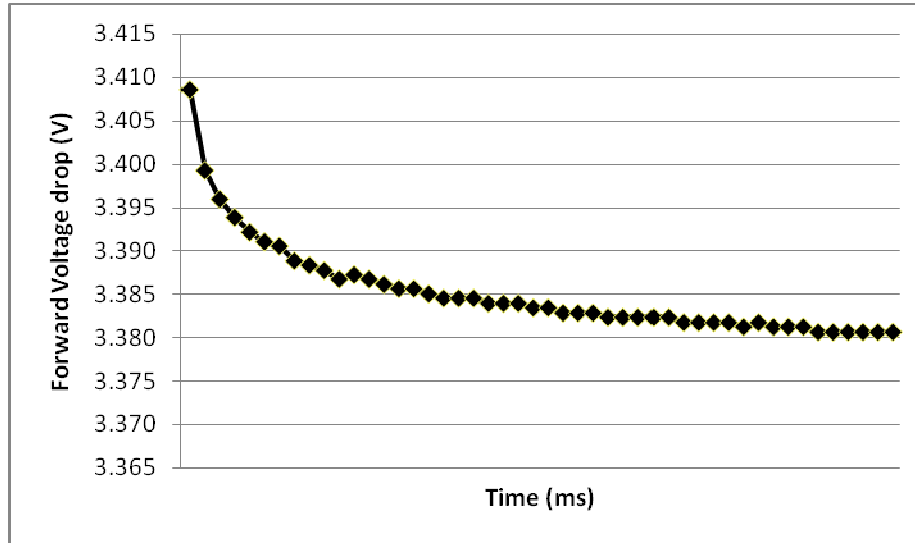
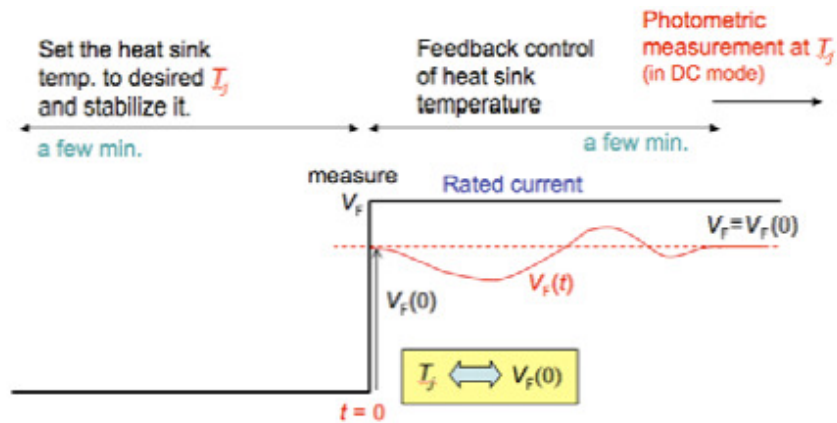
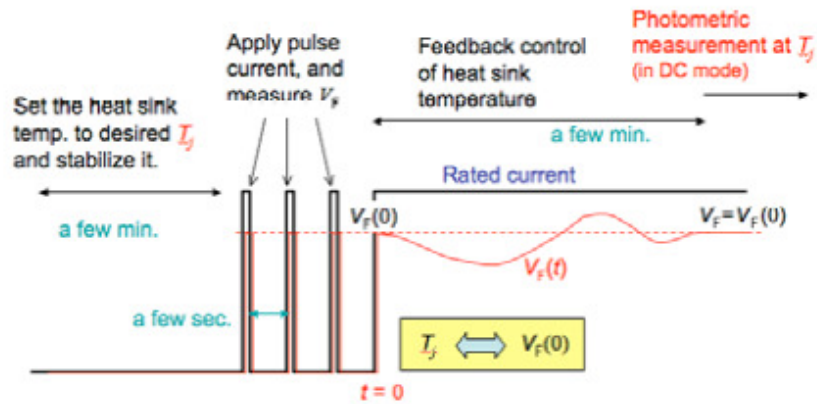


Figure 29: Forward voltage drop over time

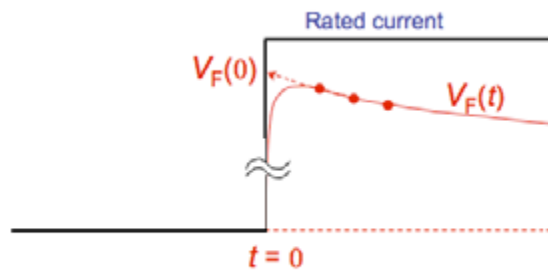
The forward voltage recovery method yield similar results that could be obtained when DC LEDs are measured using forward voltage drop method [14]. The measurement of the instantaneous voltage which is a key parameter in the experiment would be a challenge since electrical circuits will have a response time delay, measuring time delay and electrical noise during switching. Extrapolation of the instantaneous voltage would also introduce uncertainties to the measurement since heating curve has rapidly changing gradients at the initial stage as shown in Figure 29. Nevertheless the measurement method has the advantage of being independent from effects such as mounting method and thermal resistance, because it uses T_j as the reference [14]. The measurement method may also require fast measuring instruments with high resolution since voltage variations in certain types of LEDs could be very small (mV range).



(a)



(b)



(c)

Figure 30: Illustration of voltage recovery method [14].

- (a) Apply step current. (b) Apply a pulsing current. (c) Extrapolate using the heating curve

Appendix C: Pilot study to determine the uncertainty of the rms current recovery set-up

A pilot study was conducted to identify the uncertainty of the measurement set up that uses rms current recovery method to estimate T_j . This information was important in forming in experiment hypothesis. Any discrepancy in thermal resistance value estimated using the voltage drop method for AC LED and rms current recovery method should be able to explain using the measurement uncertainty of the two methods.

A calibration curve was obtained by measuring initial half cycle rms current at different temperature settings within the range of 25°C to 75°C at every 5°C increments. The objective being to replicate the initial half cycle rms current relationship with temperature as observed in the literature [2]. Since initial half cycle rms current measurement is the key temperature sensitive parameter, uncertainty of its measurement influence the T_j prediction.

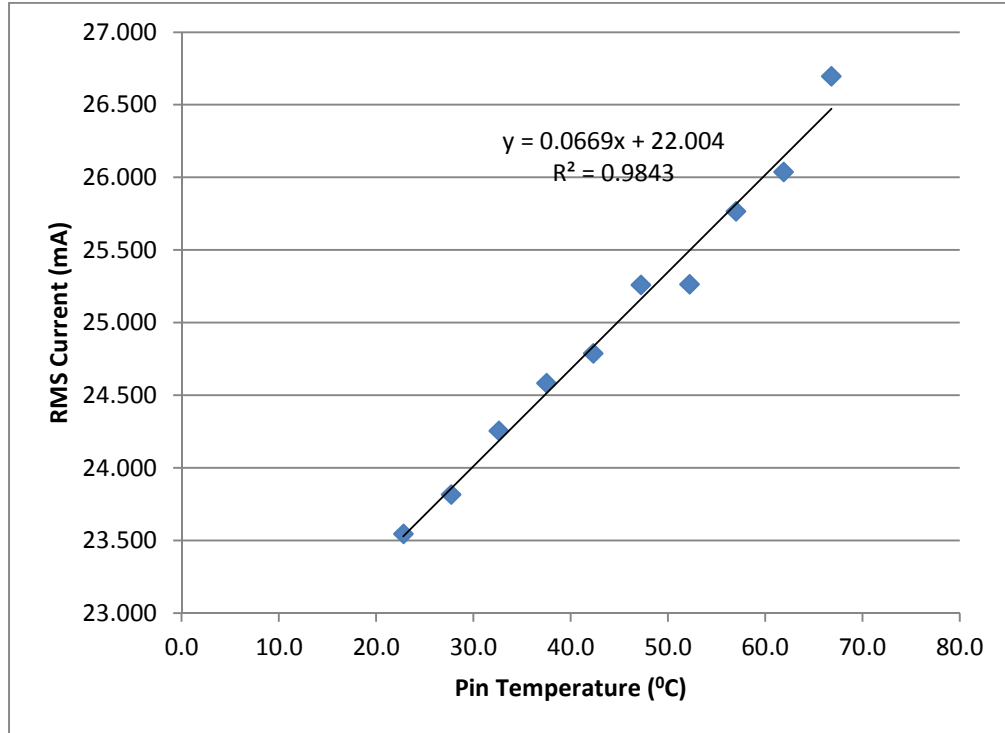


Figure 31: Frist half cycle rms current Vs. pin temperature

The calibration curve in Figure 31 shows a statistically significant correlation ($p < 0.05$) between first half cycle rms current and pin temperature as demonstrated in the literature [2]. The slope and intercept variation within a 95% confidence interval are,

$$\text{Gradient} = 0.0669 \pm 0.0033 \text{ mA}^{\circ}\text{C}$$

$$\text{Intercept} = 22.004 \pm 0.308 \text{ mA}$$

The measurement uncertainty in the calibration curve results in a 1.35°C uncertainty in the junction temperature measurement. This in turn represents $0.7^{\circ}\text{C}/\text{W}$ uncertainty (within a 95% confidence interval) in the thermal resistance measurement. This figure was further validated using repeated measurements [3]. This represents a 10% error band if thermal resistance measured using the voltage drop method for AC LED was used as the base. A detailed uncertainty analysis is provided appendix G.

Appendix D: AC LED control circuit for voltage drop method for AC LED

The custom built control circuit used in voltage drop method for AC LED performs following functions.

- Supply the AC LED with a DC calibration current and sample and hold the voltage across the AC LED at this calibration current.

The LM340-IC will act as a current regulator in providing the required reference current. Apart from the junction heating considerations the magnitude of the calibration current is limited by the fact that when it is too low the noise to signal ratio is higher, hence forth reduce the reliability of the measurement.

- Insert the reference current pulse at the desired phase angle of the AC current waveform.

The MSP430 microcontroller is programmed so that based on the control inputs provided by the user it would apply a reference DC current for calibration and an AC voltage along with a reference current pulse for measurement. The phase angle at which the reference current pulse is applied is adjustable using the software.

A Relay with a mercury wetted contact switch the current to the desired calibration current as shown in Figure 32. This transition is controlled by the MSP430 microcontroller. The voltage across the AC LED is sampled with a fixed time delay (1ms) to avoid the influence of switching electrical noise on the measurement.

The sample and hold circuit (SMP04ES) captures the sampled voltage and stores the value every time a reference current pulse is applied. At every instance a reference current pulse is applied, the sampled voltage will over write the previous value. Since the reference pulse is applied at the current dead-zone, the measured voltage across the AC LED should not change with time after AC LED reached thermal stability. In order to verify this, one hundred samples of the voltage across an AC LED at reference current were measured after reaching thermal stability under AC operating conditions. The

standard deviation of the samples was 0.4mV, which represents a standard deviation of 0.1⁰C of T_j measurement, which is within the uncertainty of the measurement setup.

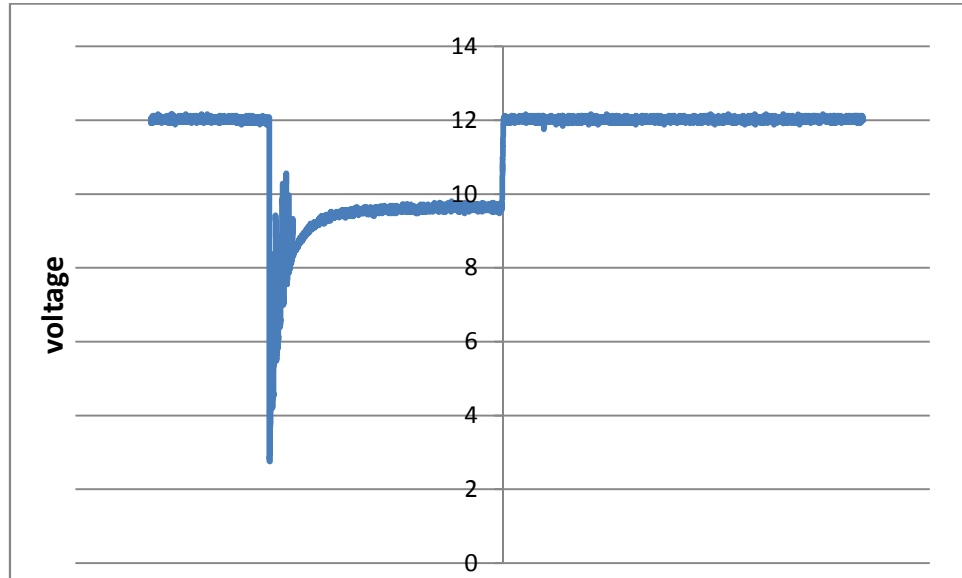


Figure 32: The reference current pulse

- The control circuit also has the ability to apply the input AC voltage waveform to the AC LED starting from any specified phase delay.

This functionality enables a user to apply an AC waveform for a short duration. For example, a user could only apply a half cycle, quarter of a cycle or a full cycle of AC voltage waveform based on his requirement. This functionality was used to plot the heating curve of the junction during the first half cycle of the AC voltage.

Appendix E: Optical power measurement

An eight inch integrating sphere along with a spectroradiometer (Ocean Optics USB 2000) was used to measure the optical power of the AC LED. The sphere set up was calibrated using three different halogen lamps that have a known spectrum measured in a NVLAP accredited integrating sphere. The calibration lamp was fully inserted to the sphere through a port and was powered using a DC power supply. A shunt resistor was used to measure the current supplied to the lamp to ensure the same current that was used to measure the spectrum of the lamp in the NVLAP sphere is used. The lamp was allowed to stabilize for 20min. Once the lamp is stabilized the raw data of the spectrum was obtained. Integration period of 5ms was used for calibration. A calibration factor graph shown in Figure 33 was obtained for each wavelength by dividing the spectrum obtained in the NVLAP sphere by the raw data obtained in the eight inch integrating sphere.

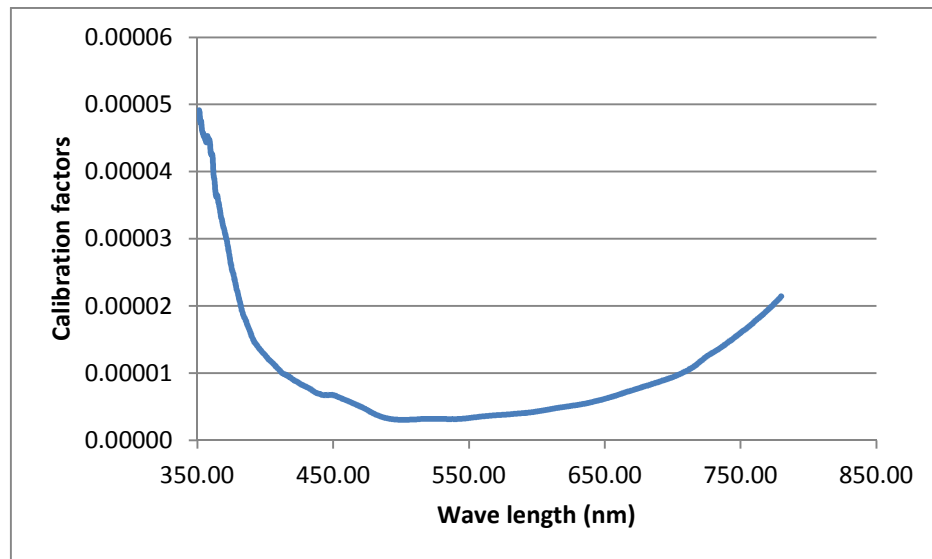


Figure 33: Calibration factors used for integrating sphere calibration

The AC LED sample attached to the thermoelectric cooler was placed next to an open port facing the interior of the sphere. The direct view of the AC LED by the fiber optic was blocked using a baffle. The area surrounding the AC LED was covered using a

white tape, without blocking the light. A spectral power distribution (SPD) of phosphor converted white AC LED obtained using the calibrated integrating sphere set up is shown in Figure 34. The optical power was obtained by integrating the SPD. Optical power was measured for all input power (110V, 120V & 130V) and temperature (25⁰C, 50⁰C & 75⁰C) conditions.

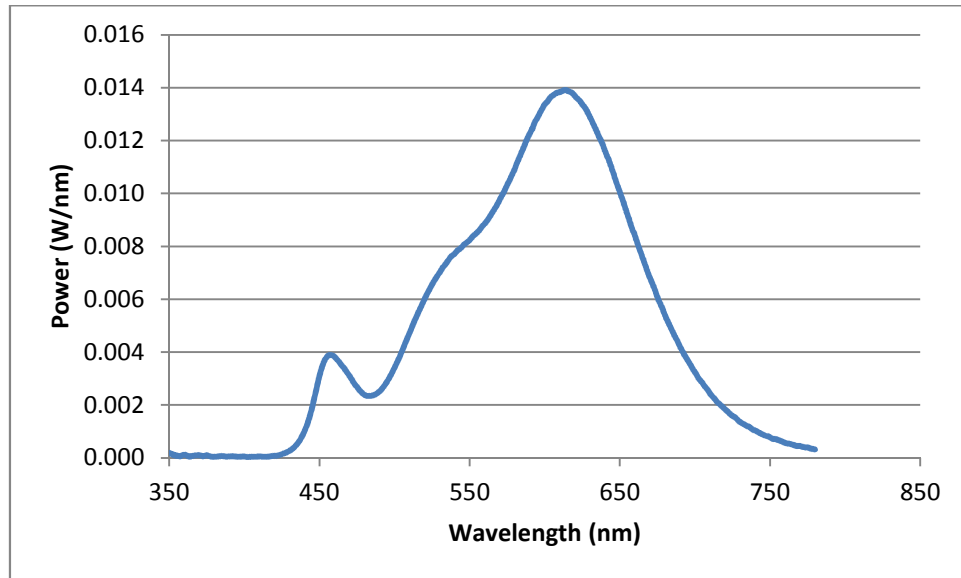


Figure 34: Spectral power distribution of a white AC LED

Optical power measurements of a GaN based white AC LED package at different cold plate temperature settings is shown in Figure 35. The optical power of the AC LED package reduces with ambient temperature and therefore influences the thermal power dissipation in the junction at different temperatures. Therefore it's important to measure optical power of a LED package at the appropriate temperature to accurately calculate thermal resistance.

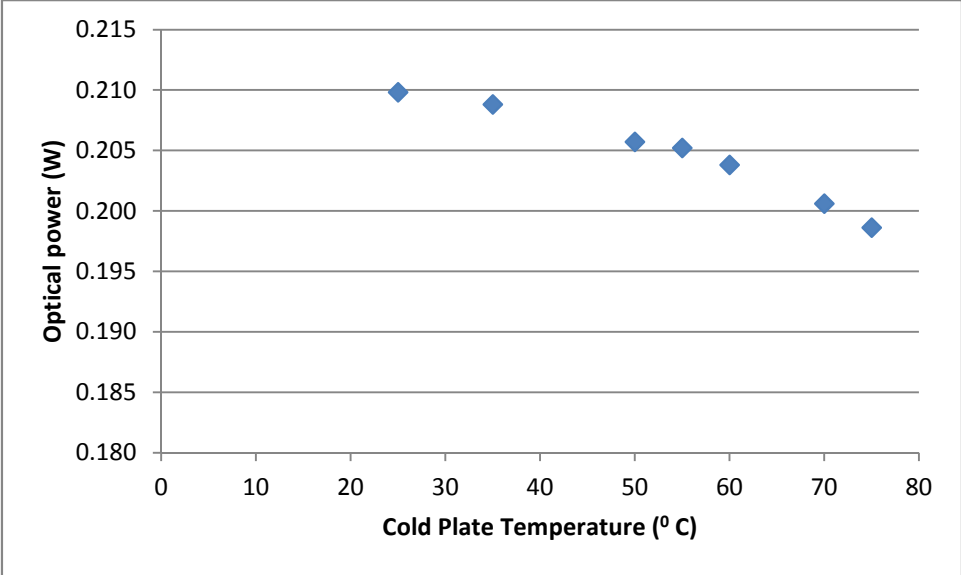


Figure 35: Variation of optical power with temperature

Appendix F: Results of Samples measured

Sample 1

The Calibration curve for sample 1, a GaN phosphor converted white AC LED is given in Figure 36.

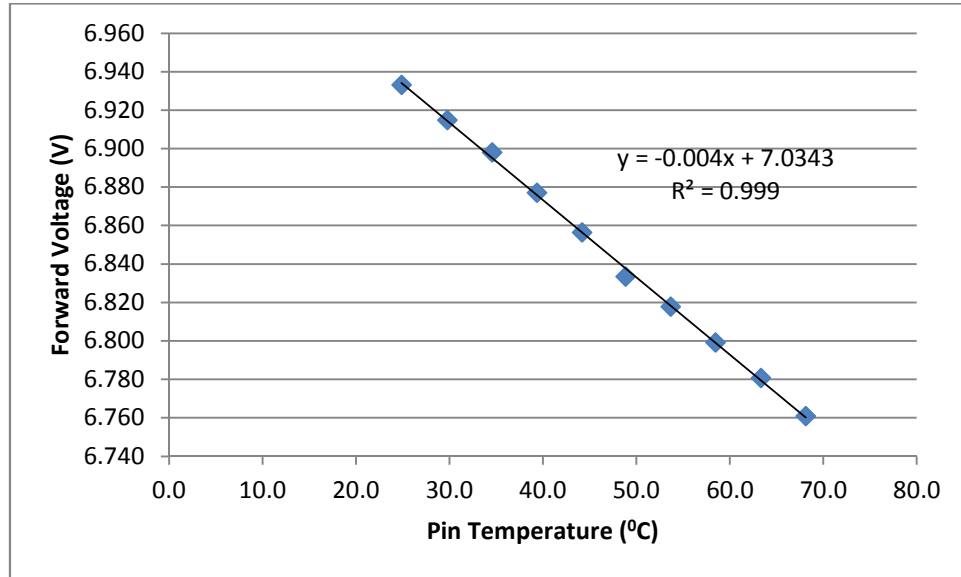


Figure 36: Calibration curve for sample 1

The average of estimated T_j measurements at each voltage and temperature combination for sample 1 is given in the following Table 16.

Input Voltage	25°C	50°C	75°C
110V	37.8°C	63.9°C	92.2°C
120V	42.9°C	70.3°C	100.1°C
130V	50.0°C	79.0°C	110.8°C

Table 16: Average of estimated junction temperature for Sample 1

The thermal resistance was calculated using following formula,

$$R_{J-P} = \frac{(\text{Junction Temperature} - \text{Pin Temperature})}{(\text{Input Electric power} - \text{optical power})}$$

The Table 17 list input electric power levels at each input voltage and temperature combinations.

	25°C	50°C	75°C
110V	1.87W	2.04W	2.22W
120V	2.79W	3.04W	3.31W
130V	3.95W	4.28W	4.59W

Table 17: Electric input power for sample 1

The optical power data at each input voltage and temperature combinations are given in Table 18.

	25°C	50°C	75°C
110V	0.166W	0.167W	0.146W
120V	0.210W	0.206W	0.199W
130V	0.219W	0.219W	0.203W

Table 18: Optical power of sample 1

Based on the above data, the thermal resistance was calculated at each input voltage and temperature combination. The average T_j value was used in calculating the thermal resistance shown in Table 19. All thermal resistance values have the units of $^{\circ}\text{C}/\text{W}$.

	25°C	50°C	75°C
110V	7.0	7.5	8.9
120V	6.4	7.1	8.3
130V	6.2	6.9	8.2

Table 19: Thermal resistance of sample 1

An F-test with a 3 x 3 factorial design was used to identify whether there is a significant impact of temperature and input AC voltage on the thermal resistance of sample 1. The results of the analysis are shown in Table 20.

Source	Type III Sum of Squares	df	Mean Square	F	Sig.
power	1.192	2	0.596	25.341	0.005
temp	13.297	2	6.649	242.833	0.000
power * temp	0.489	4	0.122	6.826	0.011

Table 20: Results of 3 by 3 F-test for sample 1

For a criterion probability of $P < 0.05$, it is clear that thermal resistance is dependent on both input power and temperature. One tail student t-test was performed to compare the means of the temperature data points for sample 1. The results of the paired test for sample 1 are given below in Table 21.

Pairs		t	df	Sig. (1-tailed)
Pair 1	110V25C - 110V50C	-5.684	2	0.015
Pair 2	110V25C - 110V75C	-7.767	2	0.008
Pair 3	110V50C - 110V75C	-7.859	2	0.008
Pair 4	120V25C - 120V75C	-7.914	2	0.008
Pair 5	120V50C - 120V75C	-10.925	2	0.004
Pair 6	120V25C - 120V50C	-4.987	2	0.019
Pair 7	130V25C - 130V50C	-25.843	2	0.001
Pair 8	130V25C - 130V75C	-244.061	2	0.000
Pair 9	130V50C - 130V75C	-55.625	2	0.000

Table 21: Results of the T-test that compared the temperature points of sample1

For a probability criterion of $P < 0.025$ (one tail t-test) all the compared means show a significant difference. This would mean that when the input AC voltage is held constant measured thermal resistance is significantly different at different cold plate temperatures.

The F-test showed that input AC voltage has a significant effect on thermal resistance. A pair wise comparison was performed between thermal resistance measured at different input AC voltages at a given cold plate temperature. Results of the t-test analysis are shown in Table 22.

		t	df	Sig. (1-tailed)
Pair 1	110V25C - 120V25C	4.551	2	0.023
Pair 2	110V25C - 130V25C	8.103	2	0.007
Pair 3	120V25C - 130V25C	3.949	2	0.029
Pair 4	110V50C - 120V50C	16.695	2	0.002
Pair 5	110V50C - 130V50C	7.879	2	0.008
Pair 6	120V50C - 130V50C	1.623	2	0.123
Pair 7	110V75C - 120V75C	-0.175	2	0.438
Pair 8	120V75C - 130V75C	0.602	2	0.304
Pair 9	110V75C - 130V75C	0.624	2	0.298

Table 22: Paired T-test for sample 1 at different input voltages

For a criterion probability of $P < 0.025$ (one tail test) part of the compared means don't show a significant difference. It is evident from the data that there is a clear thermal threshold beyond which the effect of temperature increase around the LED package nullifies the impact of reduction in thermal resistance due to high input voltage. The fact that the F-test indicated a possible interaction between temperature and AC input voltage on the thermal resistance measurement supports this argument.

Sample 2

The calibration curve for sample 2 is given below in Figure 37.

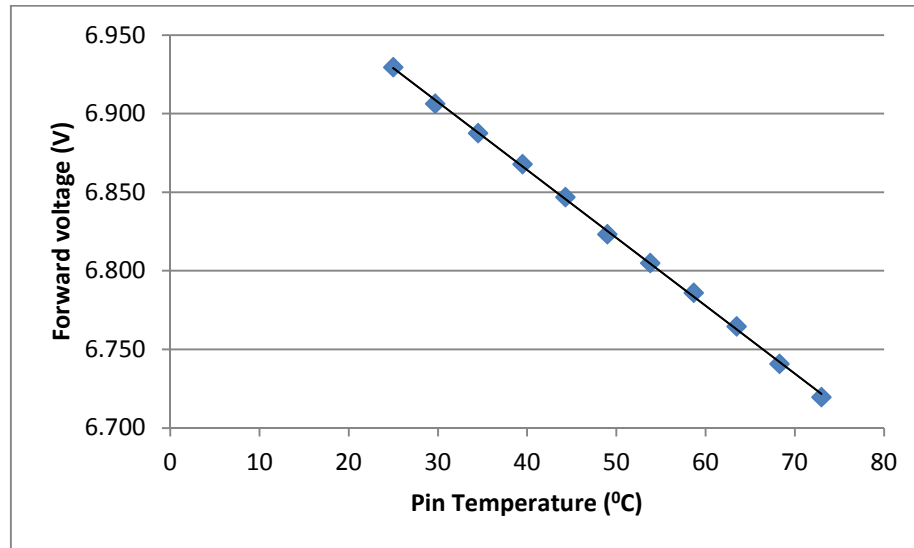


Figure 37: Calibration curve for sample 2

The T_j has strong linear correlation ($R^2 = 0.994$, $P < 0.05$) with forward voltage, therefore sample 2 satisfies the basic requirement to use the forward voltage drop method. The gradient and the intercept of the line of best fit along with their tolerances (95% confidence interval) are given below.

$$\text{Gradient} = 0.0043 \pm 0.0001 \text{ V/}^\circ\text{C}$$

$$\text{Intercept} = 7.0368 \pm 0.0041 \text{ V}$$

Junction temperature at three different AC input voltages (110V, 120V & 130V) were estimated using the calibration curve. At each input voltage the AC LED package was tested at three different temperature settings (25°C , 50°C & 75°C). At each AC input voltage and temperature combination three independent measurements were obtained. All measurements were obtained in a random order.

The average of estimated T_j at each input AC voltage and temperature combination for sample 2 is given below in Table 23.

	25 ^o C	50 ^o C	75 ^o C
110V	40.0 ^o C	67.1 ^o C	96.1 ^o C
120V	45.9 ^o C	72.4 ^o C	101.2 ^o C
130V	53.3 ^o C	81.0 ^o C	111.6 ^o C

Table 23: Estimated Junction Temperature of sample 2

The optical power data for sample 2 is given in Table 24.

	25 ^o C	50 ^o C	75 ^o C
110V	0.160W	0.160W	0.157W
120V	0.197W	0.195W	0.189W
130V	0.237W	0.229W	0.217W

Table 24: Optical power of sample 2

The electric input power data is given in Table 25.

	25 ^o C	50 ^o C	75 ^o C
110V	1.72W	1.88W	2.04W
120V	2.55W	2.77W	2.98W
130V	3.62W	3.90W	4.18W

Table 25: Electric input power of sample 2

The thermal resistance of the AC LED package was calculated based on the formula stated above. The average T_j was used to calculate thermal resistance values. All the thermal resistance values in Table 26 are in ^oC/W.

	25 ^o C	50 ^o C	75 ^o C
110V	8.0	8.8	10.7
120V	7.3	7.5	8.5
130V	6.6	7.0	8.1

Table 26: Thermal resistance of sample 2

F-test analysis shown in Table 27 demonstrates that both temperature and input AC voltage has a significant influence on the thermal resistance. The variation of thermal resistance with input voltage at different ambient temperatures is shown in Figure 38. The statistical analysis shows that “*If the ambient temperature surrounding the AC LED*

increases from 25⁰C to 75⁰C then the thermal resistance value will increase.” Therefore hypothesis 3 is verified for sample 2.

The mean thermal resistance of sample 2 showed a decreasing trend when input voltage increase from 110V to 130V. There is no significant difference between thermal resistance values measured at 120V and 130V at high ambient temperatures. Therefore the hypothesis, “If the input voltage to the AC LED increases from 110V to 130V then the thermal resistance value will decrease” is only partially verified.

Source	Type III Sum of Squares	df	Mean Square	F	Sig.
power	17.167	2	8.584	161.309	0.000
temp	15.109	2	7.555	144.607	0.000
power * temp	1.958	4	0.490	26.022	0.000

Table 27: Results of F-test analysis for sample 2

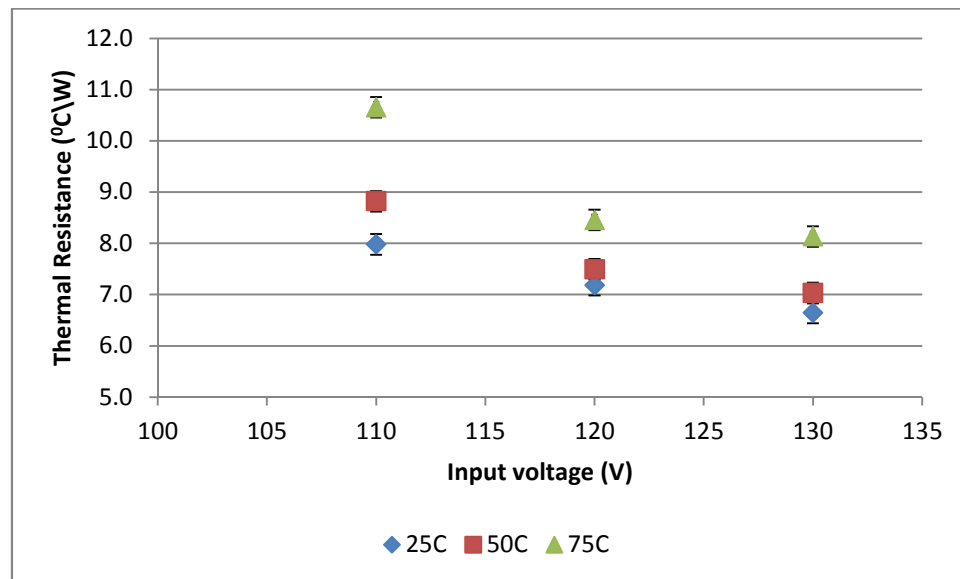


Figure 38: Variation of thermal resistance with input AC voltage for sample 2

Appendix G: Uncertainty Analysis

Propagation of error formulas [58] was used to determine the standard deviation of the T_j measurement in the voltage drop method for AC LED measurement setup.

The standard deviation of a two variable function of the form $Y = AX + BZ$ when X and Z are the averages of two variables are given as,

$$S = \frac{1}{\sqrt{N}} \sqrt{(A^2 S_x^2 + B^2 S_z^2)}$$

The standard deviation for a two variable function of the form, $y = \frac{x}{z}$, when X and Z are averages of the two variables is given as,

$$S = \frac{1}{\sqrt{N}} \times \frac{X}{Z} \times \sqrt{\left(\frac{S_x^2}{X^2} + \frac{S_z^2}{Z^2}\right)}$$

Where,

N – independent repeated measurements

S_x – Standard deviation of x

S_z – Standard deviation of z

The above formulas are generated with the assumption that X and Z are two independent variables. If they are dependent and their covariance could be reliably determined then a covariance term needs to be included in the formulas.

Voltage drop method for AC LED

Junction temperature is calculated using the calibration curve as follows,

$$T_j = \frac{(Y - C)}{K}$$

Where,

Y – Voltage measured by applying the reference current pulse during synchronized AC operation.

C- intercept of the calibration curve

K- gradient of the calibration curve

Three repeated measures of Y were obtained at different input AC voltage and temperature combinations, and to be conservative the situation where the highest standard deviation of Y was observed, was used to determine the uncertainty.

$$Y = 6.6979 \pm 0.00509V$$

$$C = 7.0325 \pm 0.0057V$$

$$K = -4.0 \pm 0.1 \text{ mV}/^{\circ}\text{C}$$

$$N = 3$$

Using the above values and formulas the uncertainty of the voltage drop method for AC LED measurement set up in estimating T_j was estimated as 1.35°C . The formula for thermal resistance is given as,

$$R_{\theta J-P} = \frac{(T_j - T_p)}{P_{net}}$$

Following values were used in the propagation of error formula (NIST, 2003).

$$T_j = 70.3 \pm 1.4^{\circ}\text{C}$$

$$T_p = 50.3 \pm 1.5^{\circ}\text{C} \text{ (standard error of a J-type thermocouple)}$$

$$P_{net} = 2.85 \pm 0.01 \text{ W (standard error of measurement instrument)}$$

The standard deviation of the experiment set up that was used to measure thermal resistance using voltage drop method for AC LED was $0.2^{\circ}\text{C}/\text{W}$. Therefore it could be stated with 95% confidence that the thermal resistance value measured using the voltage drop method using this set up for the GaN AC LED sample would be within $0.4^{\circ}\text{C}/\text{W}$ of its mean. This is approximately 5.5% of the measured value.

Rms current recovery method

A similar uncertainty analysis was performed for the rms current recovery method measurement set up. The initial half cycle rms current vs. temperature graph in Figure 31 was used to determine the uncertainty of the recovered pin temperature. Even though the T_j is not directly measured using a calibration curve in this method, the uncertainty of the recovered pin temperature is directly influenced by the uncertainty of the initial half cycle rms current and current vs. temperature relationship of the AC LED.

$$T_j = \frac{(Y - C)}{K}$$

Where,

Y - steady state rms current

C – Intercept of the initial half cycle rms current vs. temperature curve

K – sensitivity of the rms current to temperature

For Y most conservative estimate was chosen by considering the average rms current with the largest standard deviation. It is assumed that all parameters are independent.

$$Y = 25.664 \pm 0.144 \text{ mA}$$

$$C = 22.004 \pm 0.308 \text{ mA}$$

$$K = 0.0669 \pm 0.0033 \text{ mA/}^\circ\text{C}$$

Using the propagation of error formulas mentioned above it could be stated that the estimated T_j using this set up has a standard deviation of 2.3°C .

Thermal resistance is calculated as,

$$R_{\theta J-P} = \frac{(\text{Initial pin temperature} - \text{Recovered pin temperature})}{\text{Thermal input power}}$$

Using similar propagation of error formulas above with following estimates of standard deviations, the standard deviation of thermal resistance was determined.

$$\text{Initial pin temperature} = 65.8 \pm 1.5^\circ\text{C} \text{ (standard uncertainty of a J-type thermocouple)}$$

$$\text{Recovered pin temperature} = 56.9 \pm 2.3^\circ\text{C}$$

$$\text{Thermal input power} = 2.5 \pm 0.01 \text{ W}$$

The standard deviation of the thermal resistance measurement in the rms current recovery method measurement set up is 0.35°C/W . Therefore it could be stated with 95% confidence that the thermal resistance measured in this set up for the GaN AC LED sample would be within 0.7°C/W of its mean. This is approximately 10% of the measured value.

Peak wavelength shift method

The uncertainty analysis for the T_j estimated using the peak wavelength shift method yield following results.

$$T_j = \frac{(Y - C)}{K}$$

Where,

Y- peak wavelength at steady state operation

C- intercept of the calibration curve

K – gradient of the calibration curve.

For Y, as the most conservative approach, the wavelength that showed the highest standard deviation was chosen.

$$Y = 621.49 \pm 0.254 \text{ nm}$$

$$C = 615.58 \pm 0.31 \text{ nm}$$

$$K = 0.1405 \pm 0.0059 \text{ nm}/^\circ\text{C}$$

The standard deviation of the estimated T_j in the peak wavelength measurement setup was calculated as 1.4°C . Using this value the uncertainty of the overall thermal resistance measurement can be calculated. The formula used to calculate thermal resistance is given below.

$$R_{\theta J-P} = \frac{(T_j - T_p)}{P_{net}}$$

$$T_j = 42.0^\circ\text{C} \pm 1.4^\circ\text{C}$$

$$T_p = 28.0^\circ\text{C} \pm 1.5^\circ\text{C} \text{ (Standard error for J-type thermocouple)}$$

$$P_{net} = 2.31 \pm 0.01 \text{ W (Standard error for power measurement instrument)}$$

The standard deviation of thermal resistance based on the above values is $0.25^\circ\text{C}/\text{W}$. Therefore it could be stated with 95% confidence that thermal resistance measured using peak wavelength shift method measurement setup for GaP sample would be within $0.5^\circ\text{C}/\text{W}$ of its mean. This represents approximately 10% of the measured thermal resistance of the GaP based AC LED package.